



HAL
open science

Tracking asphalt markers in bitumen oil paint reconstructions by Py-TMAH-GC/MS and Py-GCxGC/MS

Raquel Marques, Michel Sablier, Jaap Boon, Gauthier Rosé, Leslie Carlyle, Isabel Pombo Cardoso, Laurence de Viguerie

► To cite this version:

Raquel Marques, Michel Sablier, Jaap Boon, Gauthier Rosé, Leslie Carlyle, et al.. Tracking asphalt markers in bitumen oil paint reconstructions by Py-TMAH-GC/MS and Py-GCxGC/MS. *Microchemical Journal*, 2022, 181, pp.107762. 10.1016/j.microc.2022.107762 . hal-03788587

HAL Id: hal-03788587

<https://hal.science/hal-03788587>

Submitted on 10 Oct 2022

HAL is a multi-disciplinary open access archive for the deposit and dissemination of scientific research documents, whether they are published or not. The documents may come from teaching and research institutions in France or abroad, or from public or private research centers.

L'archive ouverte pluridisciplinaire **HAL**, est destinée au dépôt et à la diffusion de documents scientifiques de niveau recherche, publiés ou non, émanant des établissements d'enseignement et de recherche français ou étrangers, des laboratoires publics ou privés.

Tracking asphalt markers in bitumen oil paint reconstructions by Py-TMAH-GC/MS and Py-GCxGC/MS

Raquel Marques^{*1}, Michel Sablier², Jaap J. Boon³, Gauthier Rosé^{2,4}, Leslie Carlyle¹, Isabel Pombo Cardoso¹, Laurence De Viguier⁴

¹ *Department of Conservation and Restoration and LAQV-REQUIMTE, NOVA School of Science and Technology, Universidade Nova de Lisboa, 2829-516 Caparica, Portugal*

² *Centre de Recherche sur la Conservation (CRC, USR 3224), Muséum national d'Histoire naturelle, Ministère de la Culture, CNRS, 75005 Paris, France*

³ *JAAP Enterprise for Art Scientific Research, Amsterdam (NL)*

⁴ *Laboratoire d'archéologie moléculaire et structurale, Sorbonne Universités, UPMC Univ. Paris 06, CNRS, UMR 8220, Paris, France*

*corresponding author: rd.marques@campus.fct.unl.pt

Keywords: Py-TMAH-GC/MS; Py-GCxGC/MS; Trinidad Lake Asphalt; Bitumen Oil Paint; Alligatoring

Abstract

Bitumen brown oil paint reconstructions based on 19th century production records from the British colourman Winsor & Newton were analysed using thermally assisted methylation with tetramethylammonium hydroxide (Py-TMAH-GC/MS), and pyrolysis-comprehensive two-dimensional gas chromatography (Py-GCxGC/MS). Reconstructions were compared with the starting material, Trinidad Lake asphalt (TLA), to determine how detectable this asphalt is after heat processing in lead treated linseed oil. The use of brown paint containing asphalt/bitumen (the names are used interchangeably) was blamed for severe film-forming defects in 18th and 19th century oil paintings, yet this material has rarely been identified in earlier studies of historical paintings. This research offers a possible explanation for the paucity of evidence as it reveals that asphalt markers identified in the TLA disappear in the first stage of reconstructing bitumen brown oil paint.

1. Introduction

A brown oil paint prepared from asphalt has been reported to be in widespread use in oil paintings, particularly during the 18th and 19th centuries [1,2]. Prized for its transparent deep brown tone, it was employed on its own or in glazes on top of more opaque paint, however it gained a reputation for causing paint-film defects, such as severely disfiguring drying cracks and surface distortions which came to be referred to as “Alligatoring” or “Bitumen Cracking” [3–5].

Despite the association with asphalt (or bitumen, the names were used interchangeably) only on rare occasions have chemical analyses of alligatoring proven those assumptions correct [1,6,7]. This

was thought to be due to the challenge of identifying asphalt in tiny samples from historical oil paintings. Further explanations pointed to different varieties of asphalt and the lack of precision in their identification in historical samples since this material can be sourced from many geolocations [8]. In addition, in the 19th century the use of an artificial asphalt produced from coal-tar was also reported [3,4].

Not only do asphalts in their natural form display highly complex chemical composition, this material was heavily processed prior to use as a brown pigment for artists and could have additional materials introduced during preparation and use [2,4]. Recently a series of production records for the British colourman, Winsor & Newton (W&N)'s "Bitumen Brown for Oil Paint" were analysed and a representative production was reconstructed using historically appropriate materials [9,10].

With the aim of investigating how the preparation process (cooking, boiling and the addition of different materials) may influence the ability to detect the asphalt within the final paint product, an in-depth characterization of materials from each step of the reconstruction was carried out using Py-TMAH-GC/MS and Py-GCxGC/MS. The purpose was to track asphalt feature markers throughout the reconstruction of the bitumen brown oil paint.

1.1 Asphalt/bitumen characterisation

Natural asphalt or bitumen is reported to be composed of an n-heptane soluble fraction of hydrocarbon referred to as maltene (MAL) and an insoluble fraction of polycyclic asphaltene (ASP) the latter of which has a very high molecular weight. Both fractions are responsible for the properties of the material [11].

Asphaltenes are defined as the crude-oil fraction of bitumen and are soluble in aromatic solvents (e.g., toluene or benzene) but insoluble in aliphatic solvents (e.g., n-heptane, or n-pentane). In contrast, the maltene fraction is soluble in aliphatic solvents only.

The heaviest component in bitumen, the asphaltene fraction has a strong tendency to aggregate due to the attraction between its polyaromatic fused rings. In addition to the complex mixture of hydrocarbons and asphaltenes, natural asphalts also contain resins, NSO¹ compounds and complexed metals in the form of heteroatoms: mainly vanadium and nickel [12–14].

The rich chemistry of bitumen results in a diversity of intermolecular associations which in turn facilitates the formation of nanoscale to macroscale microstructures [15]. The "Yen-Mullins model" sheds light on the molecular and colloidal structure of asphaltenes in crude oils and with laboratory solvents: in sufficient concentration asphaltene molecules form nanoaggregates, then at higher concentrations these nanoaggregates form clusters [16]. The resulting structures are responsible for the physical and mechanical properties of bitumen.

Since the chemical and physical variations in natural asphalt are dependent on the geological source, as well as on the refining methods used, there is no single precise chemical structure or chemical composition of asphalt/bitumen.

Asphalts are therefore characterized by the percentage of carbon, hydrogen, trace NSO compounds and other elements present in the mineral matter. Its chemical composition is fundamentally related to its crude source and specific biomarkers for its depositional environment (Fig. 1). In earlier studies, Raymond White used the distribution of extractable hopanes as markers for asphalt compounds in artworks [7,17], then Languri (2004) developed an analytical methodology based on mass spectrometric techniques, such as Py-GC/MS, PY-TMAH-GCMS and direct temperature-resolved mass spectrometry (DTMS), amongst others, for the characterization of a large number of biomarkers and marker compounds with the aim of detecting these markers in 19th century reference materials, model

¹ Nitrogen, sulphur and oxygen compounds.

systems and historical paintings suffering from film-forming defects. An asphalt sample from the 19th Century Hafkenscheid collection was investigated with mass spectrometric techniques [18]. Py-GC/MS revealed alkanes and alkenes, a number of alkyl-aromatic compounds and alkylbenzothiophenes plus a few compounds with hopane carbon skeletons, gammacerane and C-ring monoaromatic steroids. Asphalts contain many different sulphurised lipids but their detection requires chemical reduction techniques, which are hard to do on microsamples such as from paintings. The various alkylbenzothiophenes are however indirect indicators for the presence of (poly)sulphide bridges in asphaltic complex materials [19]. The distribution of the pyrolysis products of asphalts were used by Languri (2004 chapter 5) to investigate how the asphalt markers are affected by paint manufacturing processes. The effects of roasting of asphalt, solvent extraction, addition to drying oils and their accelerated aging were investigated. Further changes in asphalt paint composition can result from oxidative conditions during natural aging of the painting, and due to exposure to solvent-based restoration treatments, which can extract solvent sensitive materials such as the maltene fraction. Languri however only investigated some of the effects of paint making in separate experiments.

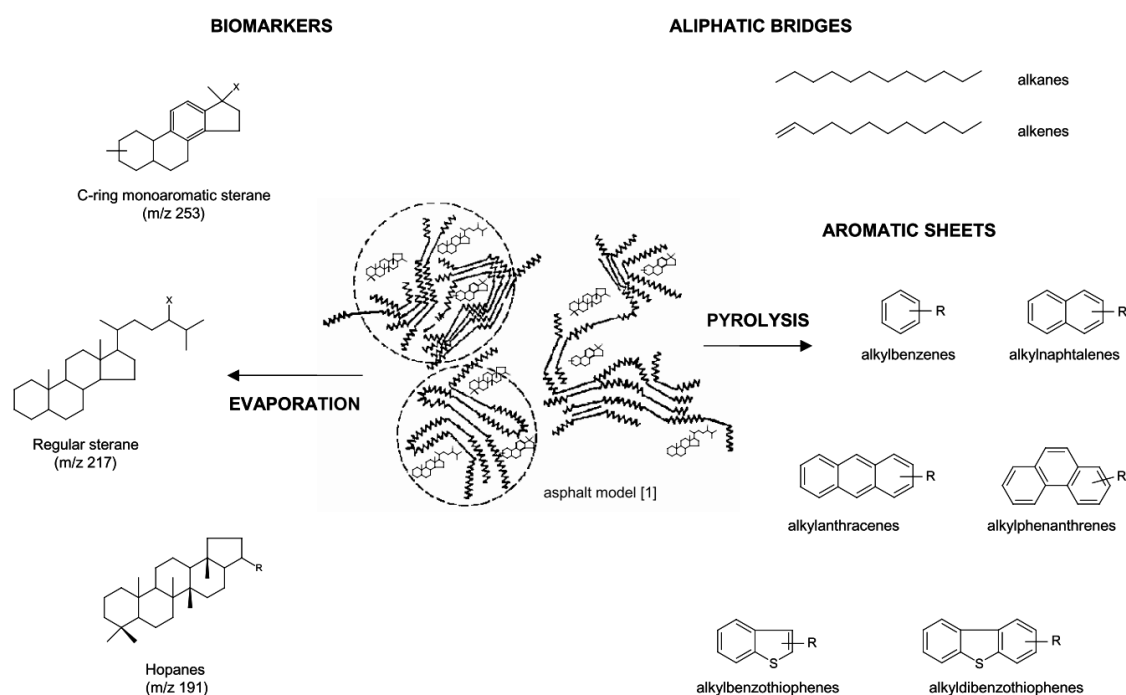


Figure 1: Reproduction of Languri's scheme, with "Yen's model" in the center surrounded by markers and biomarker molecules present in asphalt [5]. This schematic however underestimates the significance of sulphur bridges as cross links and the sulphurisation of lipid biomaterials [20].

1.2 Py-TMAH-GC/MS and Py-GCxGC/MS

Pyrolysis gas chromatography/mass spectrometry (Py-GC/MS) offers a high degree of sensitivity for organic components in small samples of complex materials found in historical cultural objects. On-line pyrolysis does not require wet chemical workup, has a low sample requirement and has been successful in the characterization of oil derived constituents after chemical drying (e.g. [21,22]). The addition of tetramethylammonium hydroxide (TMAH) allows on-line methylation of acidic compounds, ester bound substances and free alcoholic moieties. Py-TMAH-GC/MS is therefore capable of analyzing fatty acids as methyl esters released from cross-linked as well as non-crosslinked

materials (free- and esterified fatty acids), which makes separation and identification of more complex oxidised fatty acids a suitable approach [21]. Without TMAH, free fatty acids, acylglycerides and the fatty acids eliminated from the cross-linked network are much more difficult to separate effectively by gas chromatography. Elimination of fatty acids from a cross linked oil during pyrolysis can lead to an aromatised residual network that will produce various types of aromatic compounds at higher analysis temperatures [21].

Pyrolysis-comprehensive two-dimensional gas chromatography (Py-GCxGC/MS) has recently been introduced in the study of cultural heritage materials for its analytical capabilities [23–25]. This technique uses two capillary columns connected via a modulation system to optimize the complementary separation capabilities of columns of different polarities. It offers higher resolution, peak separation capacity, and selectivity and a lower detection limit for the analysis of volatile organic molecules [26]. For this research it offered a complementary technique to Py -GC/MS alone as it ensures the detection of all targeted markers.

2. Experimental

2.1 Materials and Paint Samples

Materials

TMAH: Tetramethylammonium hydroxide solution, 25 wt.% in H₂O. Linear Formula: (CH₃)₄N(OH). Supplier: Sigma-Aldrich. 331635. <https://www.sigmaaldrich.com/PT/en/product/sial/331635>

FA-C13 Internal Standard: Tridecanoic acid, analytical standard. Linear formula: CH₃(CH₂)₁₁CO₂H. Supplier: Sigma-Aldrich. 91988. <https://www.sigmaaldrich.com/PT/en/product/sial/91988>

Asphalt: Trinidad Lake Asphalt (**TLA**) was selected as the asphalt source for the reconstructions because of its extensively characterized composition (e.g. [27]), it was readily available in small quantities and had been used in previous reconstructions of bitumen brown oil paint by Bothe (1999) and Izat (2001) (see [10]). Supplier: Trinidad Lake Asphalt, Trinidad Epuré, Carl Ungewitter, Trinidad Lake Asphalt, GmbH & Co. KG, 28195 Bremen, Bgm.-Smidt-Straße 56. Germany.

Bitumen Brown Paint Samples

Reconstructions were made following the W&N production record for their bitumen brown oil paint dated 1858 (see [9] for analysis of the production records, and [10] for details on the reconstruction). The London based company first cooked ingredients together at their manufactory in Kentish Town (**KT**), then completed the recipe the next day at their premises at Rathbone Place (**RP**) see Figure 2.

W&N incorporated other previously prepared products in their bitumen brown. These were made separately for the reconstruction following their production records for Strong Drying Oil, Double

Mastic Varnish and Purple Lake pigment. The production record for their Burnt Sugar of Lead was not clear, therefore a laboratory grade lead (II) acetate trihydrate was used instead.

Following the steps in W&N’s record, asphalt was first melted into their Strong Drying Oil (linseed oil previously cooked with litharge and red lead) while heating. Burnt Sugar of Lead (refined lead acetate ground in raw linseed oil) was then added with further cooking to a maximum temperature of 318°C. After cooling, concentrated Mastic Varnish, Purple Lake pigment and Turpentine were added (resulting in the KT product). The next day, at room temperature a 1:1 proportion of the artist’s gelled medium Megilp was ground into the mixture which resulted in their final product (the RP product). Megilp was sold by W&N and other British colourmen throughout the 19th century. It was a gel formed by mixing lead-treated linseed oil and mastic resin which was used to enhance the flow properties and transparency of artist’s oil paint [4,28].

All together 15 samples were taken at different stages throughout the preparation before and after new materials were introduced (see Fig. 2). A reference sample of the Trinidad Lake Asphalt (TLA) and three selected samples from the reconstruction (see Table 1) were analysed with Py-TMAH-GC/MS and Py-GCxGC/MS.

The Bitumen Brown production record was reconstructed several times with analyses carried out on two separate reconstructions. Given the similarity in results, this paper reports on only one reconstruction.

Table 1: Sample code and description of selected samples from the reconstruction of W&N’s “Bitumen” (1858).

Sample Code	Description
KT-I	Kentish town (KT) initial (I) mixture: Strong Drying Oil + Asphalt (TLA) + Sugar of Lead after reaching ~318°C and cooking for 1h30min.
KT	Kentish Town (KT) product: which includes the mixture above with the additions of Double Mastic Varnish, Purple Lake pigment, and Turpentine. (total preparation time 2 hours).
RP	Rathborne Place (RP) final brown oil paint which includes the KT product with the addition of Megilp (1:1 strong drying oil : double mastic varnish) in a 1:1 proportion. This is the brown oil paint which was put into W&N’s paint tubes.



Figure 2: Schematic showing the sequence of samples taken during the production of W&N’s Bitumen Brown oil paint with the time and temperatures reached.

2.2 Sample Preparation for analyses

On-line: thermally assisted methylation. After adding 3 μ l of tetramethylammonium hydroxide (TMAH) in methanol (5%) with tridecanoic acid (FA-C13) as internal standard (the concentration of FA-C13 is 16 μ g/ml), the sample is homogenized and then placed in a stainless steel cup (Frontier Lab Disposable Eco-Cup SF).

2.3 Analytical Procedures

Pyrolysis transesterification gas chromatography/mass spectrometry (Py-TMAH-GC/MS). The pyrolysis unit used was a Frontier Lab 3030D pyrolyser mounted on a Thermo Scientific Trace 1310 GC / ISQ mass spectrometer combination. The analytical column was directly coupled to the pyrolyser via a home-made split device. A SLB5 ms (Supelco) column was used (length 20 m, int. diameter 0.18 mm, film thickness 0.18 μ m). Helium was used as carrier with a programmed pressured flow of 0.7-1.2 ml/min and split ratio of 1:30. The pyrolysis temperature was 480 °C. The temperature program was the following: 35 °C (1.5 min), heating at 60 °C/min to 100 °C, heating at 14 °C/min to 250 °C, heating at 6 °C/min to 315 °C (2 min). The column was directly coupled to the ion source of the mass spectrometer. The temperature of the interface and the ion source was 270 °C and 220 °C, respectively. Mass spectra were recorded from 29 until 600 amu with a speed of 7 scans per second. Xcalibur 2.1, AMDIS 2.73 and GCMSSolution (version 4.45) software were used for collecting and processing of the data.

Pyrolysis-comprehensive two-dimensional gas chromatography/mass spectrometry (Py-GCxGC/MS).

Py-GCxGC/MS analysis was conducted with a Shimadzu QP 2010 Ultra mass spectrometer (Shimadzu, Champs-sur-Marne, France) equipped with a two-stage thermal modulator ZX 2 (Zoex, Houston, USA). Pyrolysis was performed using a vertical micro-furnace-type pyrolyzer PY-3030D (Frontier Lab, Fukushima, Japan) directly connected to the injection port of the gas chromatograph. Before being placed in a stainless-steel sample cup, the samples were weighted with an XP2U Ultra Micro Balance (Mettler Toledo, Viroflay, France). Typical quantities of samples ranged from 25 to 80 μ g. The sample cup was placed on top of the pyrolyzer at near ambient temperature and was introduced into the furnace at an optimized temperature of 600°C, and then the temperature program of the gas chromatograph oven was started. The pyrolyzer interface was held at 320°C. An Optima-5HT column (30 m \times 0.25 mm I.D., 0.25 μ m film thickness, Macherey-Nagel, Hoerd, France) was used as the first dimension column and a Zebron ZB-50 (2.8 m \times 0.1 mm I.D., 0.1 μ m film thickness, Phenomenex, Le Pecq, France) was used as a second-dimension column and for the loop modulator system. The separation was carried out at an initial constant pressure of 300 kPa in the constant pressure mode, using Helium Alphagaz 2 as carrier gas (Air Liquide, Bagneux, France). The ZX 2 two-stage thermal modulator employs a closed cycle refrigerator/heat exchanger to produce a -90°C cooled air jet regularly modulated with a pulsed hot air jet. The optimized modulation period for two-dimensional chromatogram collection was 6 s to 8 s with a programmed hot pulse of 0.350 s. The modulation time was optimized depending on the distribution of chromatographic peaks in the two-dimensional chromatogram. For the ease of reading, when a modulation time of 6 s was applied, a shift phase of -2.0 s was applied during the treatment of data with the GC Image software. A multi-step temperature program was used for the hot jet set at 200°C for 30 min and subsequently raised to 280°C until the end of the acquisition. The oven temperature was initially held 1 min at 81°C, and then ramped at 3°C min⁻¹ to 325°C, where it was held for 25 min. The total duration of GC analysis was

ca. 107 min. The injector was held at 280°C and used in split mode (1:30 of the total flow). The mass spectrometer was operated at 20,000 u.s⁻¹, with a scan range from 50 to 500 u, using electron ionization at 70 eV. The interface was kept at 300°C and the ion source at 200°C. Data processing of the 2D raw data was achieved using GC Image software, version 2.4 (Lincoln, Nebraska). Identification of components was performed by comparing the mass spectra of unknown components with reference compounds from the NIST MS library (2011) and interpretation of the main fragmentations.

3. Results and Discussion

3.1 Py-TMAH-GC/MS

3.1.1 Asphalt features in the Trinidad Lake Asphalt reference sample

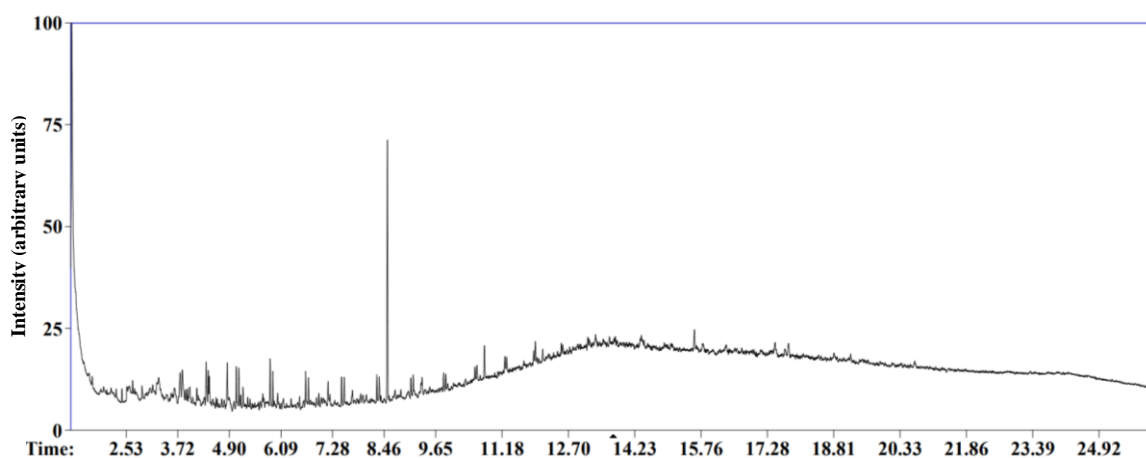


Figure 3: Total ion chromatogram (TIC) of the Trinidad Lake Asphalt reference, derivatized with TMAH.

The raw Trinidad Lake asphalt (TLA) was characterized first to serve as the reference material using the same experimental conditions which would be used later for samples from the individual steps in the reconstruction. Py-TMAH-GC/MS analysis showed a series of typical markers and biomarkers. These were defined as features to be tracked in the oil paint reconstruction samples (see Fig. 3 and Table 2).

The markers identified were the aliphatic cross-links such as the homologous series of alkanes and alkenes, the aromatic sheet compounds such as the alkylbenzenes, alkyl-naphthalenes and alkylbenzothiophenes and for the biomarkers the monoaromatic steroids, the hopane homologues (Ts, Tm, H₂₉) and the gammacerane (see Fig. 1). Languri successfully identified these features in an asphalt sample described as “asphalt rich material (...) quite similar in its properties to the asphalt from the Dead Sea” and reported on their presence or absence in asphalt oil paint reconstructions and brown layers in paint samples from selected 19th century oil paintings with drying defects [5].

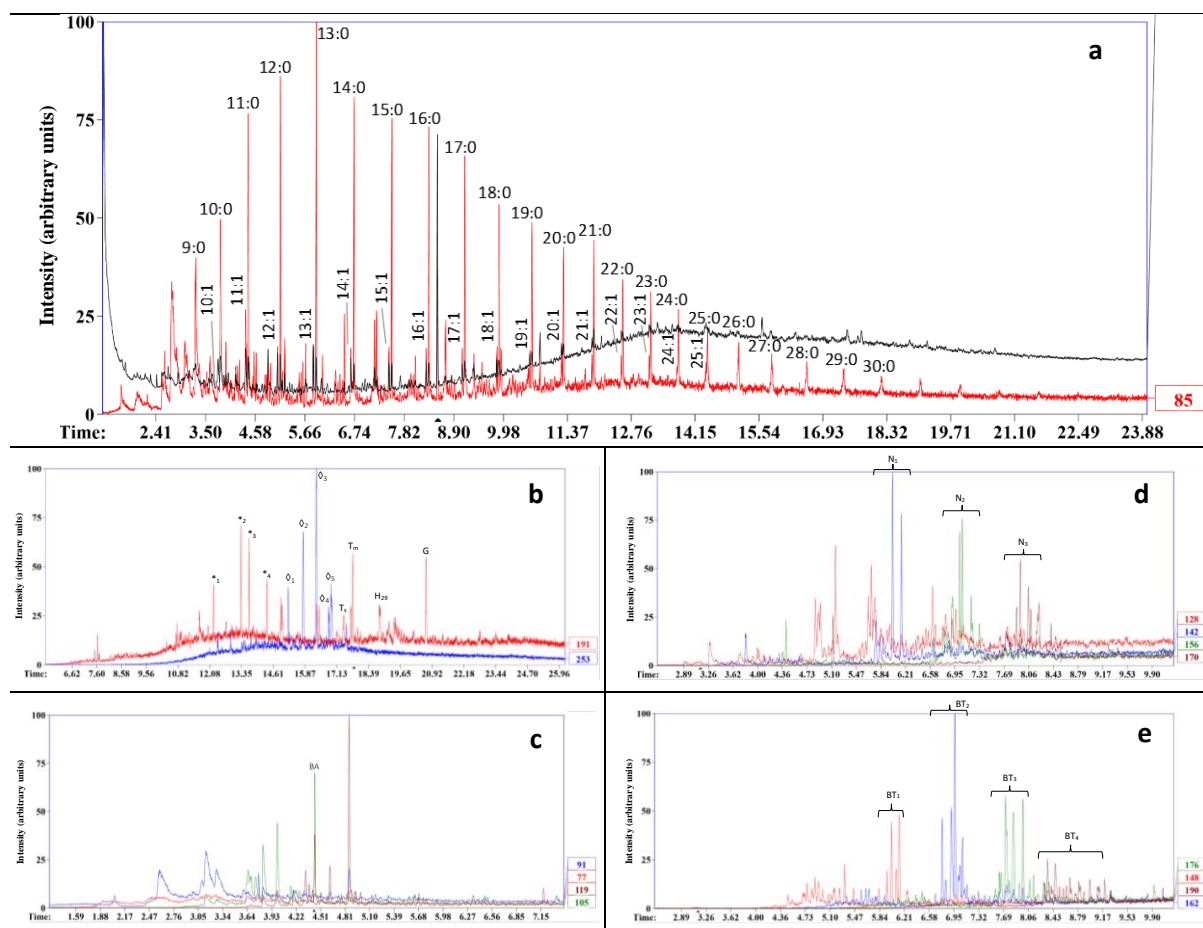


Figure 4: Mass chromatograms of TLA reference sample: a) TIC (in black), alkanes and alkenes (m/z 85, in red), b) biomarker hopanes (m/z 191 in red) and C-ring monoaromatic steroids (m/z 253 in blue); Partial mass chromatogram of: c) alkybenzenes (m/z 91, 77, 105, 119), d) alkylnaphthalenes (m/z 128, 142, 156, 170) and e) alkylbenzothiophenes (m/z 148, 162, 176, 190). Label information in Table 2.

Alkanes ranging from C9 to C30 and alkenes from C10:1 to C25:1 identified by mass peaks m/z 85 and 83 respectively have a right-skewed distribution and are a predominant feature in the TLA sample (Fig. 4 a)). The acyclic isoprenoids, pristane and phytane were not detected. Their absence might be due to biodegradation processes which can alter or remove them completely [12]. Low values of pristane/phytane ratios in Trinidad Lake asphalts have been reported along with a predominance of even homologues of *n*-alkanes. This was seen to be pointing to “a severe reducing depositional environment of the marine organic matter of carbonate facies and bitumen immaturity” [29].

The labels used to identify each component in the following markers and biomarkers were based on the work of Languri [5]. Therefore the identification of the aromatic sheet compounds has been divided into three categories: the alkybenzenes, the alkylnaphthalenes and the alkylbenzothiophenes.

For the alkybenzenes a partial mass chromatogram with m/z 77, 91, 105 and 119 mass fragments shows a few peaks of interest (Fig. 4 c)) however only the benzoic acid methyl ester (BA) was unequivocally identified. The alkylnaphthalenes are identified in Figure 4 d) for a range of peaks with m/z 142, 156, 170 respectively. This choice of a broader identification is due to the isomers present around the main peaks. The peaks for m/z 128 are present with a similar profile to the one observed in the literature [5], however, the naphthalene peak was not unequivocally identified.

The same broader identification was made for the alkylbenzothiophenes with BT₁, BT₂, BT₃ and BT₄ representing a range of peaks with m/z 148, 162, 176 and 190 respectively (see Fig. 4 e)). The presence of sulphur containing compounds such as the benzothiophenes and the dibenzothiophenes (not shown but also identified) are characteristic of the asphaltic nature of the sample and can be an indication for the geological origin of the asphalt [5]. Kohnen (1991) identified a large number of biomarker sulphur compounds and biomarker alkylthiophenes after desulpherisation using chemical workup of asphalts and kerogens from rocks. Alkylthiophenes are therefore a marker for sulphurised organic matter when analytical pyrolysis is used.

The mass chromatograms of m/z 191 and m/z 253 (Fig. 4 b)) show the characteristic fragment ions of the biomarkers hopanoid and steroid compounds identified in Table 2.

Using the mass chromatogram of m/z 191 four tricyclic terpanes and some tentatively assigned hopanoids were identified (see Fig. 4 b) and Table 2). The assignment of 18 α (H)-22,29,30-trisnorneohopane (Ts) was based on the ion fragments 191 and 368, while the 17 α (H)-22,29,30-trisnorhopane (Tm) had the m/z 191 and 370 [5]. Based on the relative retention time of the peak, and presence of fragments at m/z 191, 177, 398 [30] the compound 17 α (H),21 β (H)-30-hopane (marked as H₂₉) was tentatively identified. The assignment of gammacerane (G) was based on the retention time and the mass spectra from Nytoft where the main ion fragments seen are m/z 191 and 412 [31].

The distribution of the C-ring monoaromatic steroids is easily detected using the mass chromatogram of m/z 253 (Fig. 4 b) and Table 2). The peaks labelled ϕ_1 , ϕ_2 and ϕ_5 could be tentatively assigned to the C-ring monoaromatic steroids (MA) MA₂₇, MA₂₈ and MA₂₉ respectively based on their peak profile from the m/z 253 mass chromatogram (Fig. 8) which have a distribution consistent with the data from the literature [5,32]. Definite assignments of structures is however difficult and to achieve total certainty on this assignment it would be necessary to use standards along with the high-resolution capillary gas chromatography columns [12,32]. For this reason, these compounds remained defined as C-ring monoaromatic steroid hydrocarbons in the following table.

Table 2: List of feature compounds identified in the TLA reference sample, divided according to the classes of compounds with the respective retention time, label, formula and molecular weight. The presence (X) or absence (-) of these features in the reconstruction samples is indicated in the last three left columns.

RT (min)	Label	Compound	Formula	M.W.	TLA	KT-I	KT	RP
Alkane (m/z 57, 85) & Alkene (m/z 55, 85)								
3.28	9:0	Nonane	C ₉ H ₂₀	128	X	-	-	-
3.77	10:1	1-Decene	C ₁₀ H ₂₀	140	X	-	-	-
3.82	10:0	Decane	C ₁₀ H ₂₂	142	X	-	-	-
4.37	11:1	1-Undecene	C ₁₁ H ₂₂	154	X	-	-	-
4.42	11:0	Undecane	C ₁₁ H ₂₄	156	X	-	X	-
5.06	12:1	1-Dodecene	C ₁₂ H ₂₄	168	X	-	-	-
5.12	12:0	Dodecane	C ₁₂ H ₂₆	170	X	X	X	-
5.84	13:1	1-Tridecene	C ₁₃ H ₂₆	182	X	-	-	-
5.90	13:0	Tridecane	C ₁₃ H ₂₈	184	X	X	X	X
6.66	14:1	1-Tetradecene	C ₁₄ H ₂₈	196	X	-	-	-
6.72	14:0	Tetradecane	C ₁₄ H ₃₀	198	X	X	X	X
7.49	15:1	1-Pentadecene	C ₁₅ H ₃₀	210	X	-	-	-
7.54	15:0	Pentadecane	C ₁₅ H ₃₂	212	X	X	X	X

8.29	16:1	1-Hexadecene	C ₁₆ H ₃₂	224	X	-	-	-
8.35	16:0	Hexadecane	C ₁₆ H ₃₄	226	X	X	X	-
9.08	17:1	1-Heptadecene	C ₁₇ H ₃₄	238	X	-	-	-
9.13	17:0	Heptadecane	C ₁₇ H ₃₆	240	X	X	X	X
9.83	18:1	1-Octadecene	C ₁₈ H ₃₆	252	X	-	-	-
9.87	18:0	Octadecane	C ₁₈ H ₃₈	254	X	-	-	-
10.55	19:1	1-Nonadecene	C ₁₉ H ₃₈	266	X	-	-	-
10.60	19:0	Nonadecane	C ₁₉ H ₄₀	268	X	-	-	-
11.23	20:1	1-Eicosene	C ₂₀ H ₄₀	280	X	-	-	-
11.28	20:0	Eicosane	C ₂₀ H ₄₂	282	X	-	-	-
11.90	21:1	1-Heneicosene	C ₂₁ H ₄₂	294	X	-	-	-
11.94	21:0	Heneicosane	C ₂₁ H ₄₄	296	X	-	-	-
12.54	22:1	1-Docosene	C ₂₂ H ₄₄	308	X	-	-	-
12.57	22:0	Docosane	C ₂₂ H ₄₆	310	X	-	-	-
13.15	23:1	1-Tricosene	C ₂₃ H ₄₆	322	X	-	-	-
13.16	23:0	Tricosane	C ₂₃ H ₄₈	324	X	-	-	-
13.75	24:1	1-Tetracosene	C ₂₄ H ₄₈	336	X	-	-	-
13.78	24:0	Tetracosane	C ₂₄ H ₅₀	338	X	-	-	-
14.37	25:1	1-Pentacosene	C ₂₅ H ₅₀	350	X	-	-	-
14.41	25:0	Pentacosane	C ₂₅ H ₅₂	352	X	-	-	-
15.09	26:0	Hexacosane	C ₂₆ H ₅₄	366	X	-	-	-
15.81	27:0	Heptacosane	C ₂₇ H ₅₆	380	X	-	-	-
16.57	28:0	Octacosane	C ₂₈ H ₅₈	394	X	-	-	-
17.37	29:0	Nonacosane	C ₂₉ H ₆₀	408	X	-	-	-
18.20	30:0	Triacontane	C ₃₀ H ₆₂	422	X	-	-	-
Tricyclic Terpanes (m/z 191)								
12.23	* ₁	Tricyclic alkyl hydrocarbon (C ₂₁ ?*)		290	X	-	-	-
13.33	* ₂	Tricyclic alkyl hydrocarbon (C ₂₃ ?*)		318	X	-	-	-
13.65	* ₃	Tricyclic alkyl hydrocarbon (C ₂₄ ?*)		332	X	-	-	-
14.35	* ₄	Tricyclic alkyl hydrocarbon (C ₂₅ ?*)		346	X	-	-	-
Hopanoids (m/z 191)								
17.41	T _s	18 α (H)-22,29,30-trisnorneohopane	C ₂₇ H ₄₆	368	X	-	-	-
17.45		25,28,30-trisnorhopane	C ₂₇ H ₄₆	370	?			
17.76	T _m	17 α (H)-22,29,30-trisnorhopane	C ₂₇ H ₄₆	370	X	?	-	-
18.84	H ₂₉	17 α (H),21 β (H)-30-nor-hopane	C ₂₉ H ₅₀	398	X	?	-	-
Terpanes (m/z 191, 412)								
20.67	G	Gammacerane	C ₃₀ H ₅₂	412	X	?		
Steroids (m/z 253, 231, 245)								
15.20	\diamond_1	C-ring aromatic steroid hydrocarbon			X	-	-	-
15.80	\diamond_2	C-ring aromatic steroid hydrocarbon			X	-	-	-
16.33	\diamond_3	C-ring aromatic steroid hydrocarbon			X	-	-	-
16.80	\diamond_4	C-ring aromatic steroid hydrocarbon			X	-	-	-
16.92	\diamond_5	C-ring aromatic steroid hydrocarbon			X	-	-	-
17.68		Triaromatic steroid hydrocarbon		368	?			
Aromatics								
Alkylbenzenes (m/z 77, 91, 105, 119)								
4.44	BA	Benzoic acid methyl ester	C ₈ H ₈ O ₂	136	X	X	X	X
Alkyl naphthalenes (m/z 128, 142, 156, 170)								
~ 5.70	N ₁	C ₁ -naphthalene	C ₁₁ H ₁₀	142	X	?	?	
~ 7.02	N ₂	C ₂ -naphthalene	C ₁₂ H ₁₂	156	X	-	-	-
~ 7.93	N ₃	C ₃ -naphthalene	C ₁₃ H ₁₄	170	X	-	-	-

Alkylbenzothiophenes (m/z 148, 162, 176, 190)								
~ 6.13	BT ₁	C ₁ -benzothiophene	C ₉ H ₈ S	148	X	-	-	-
~ 6.97	BT ₂	C ₂ -benzothiophene	C ₁₀ H ₁₀ S	162	X	-	-	-
~ 7.84	BT ₃	C ₃ -benzothiophene	C ₁₁ H ₁₂ S	176	X	-	-	-
~ 8.50	BT ₄	C ₄ -benzothiophene	C ₁₂ H ₁₄ S	190	X	-	-	-

*based on [12].

N₁ = C₁ - methyl substitute; N₂ = C₂ – dimethyl substitutes; N₃ = C₃ – trimethyl substitutes

3.1.2 Asphalt features in the Reconstruction

Results obtained from sample KT-I, which was taken after cooking the asphalt with the lead-treated linseed oil (Strong Drying Oil) to a top temperature of 318°C, are detailed below, and clearly show the absence of markers and biomarkers from asphalt. As a result samples from KT and RP are not discussed further in this paper since asphalt markers will also be absent in these samples. A summary of the results obtained for KT and RP using both Py-TMAH-GC/MS and Py-GCxGC/MS can be found in Table 2, and Table S1 in the Supplementary Material (SM).

Concerning the asphalt features (Fig. 5), analyses revealed an almost complete absence of the alkanes and alkenes envelope with only C12 to C17 present. Using the mass chromatograms of m/z 191 no similar pattern to the TLA reference sample is observed in the KT-I sample. Only three peaks (with very low intensity) are present that match the retention time of the peaks identified in the TLA samples as Tm, H29 and G. However since these peaks in the KT-I sample present discrepancies when comparing their m/z values, a proper identification is unreliable. No peaks matching the TLA reference distribution of the C-ring monoaromatic steroids were detected using mass chromatography of m/z 253.

As suggested by previous thorough characterizations of differently processed linseed oil [21,33], aromatic compounds could also have been produced by the pyrolysis of the oil, despite the use of TMAH. This requires further investigation using Py-GC/MS of linseed oil processed by heating. Without TMAH, various alkyl aromatics are present in the Py-GC/MS of linseed oil paint [21] which can be explained as thermal degradation of a residual substance after elimination of fatty acids from the oil paint network.

While only benzoic acid is present among the alkylbenzenes, in the alkylnaphthalenes (previously coded N1-N3) two main peaks from the N1 group appear (with the same retention time but very little intensity). It is important to note that the alkylbenzothiophenes, which are important sulphur containing compounds characteristic of certain asphalts, have completely disappeared in the analytical data from the KT-I sample.

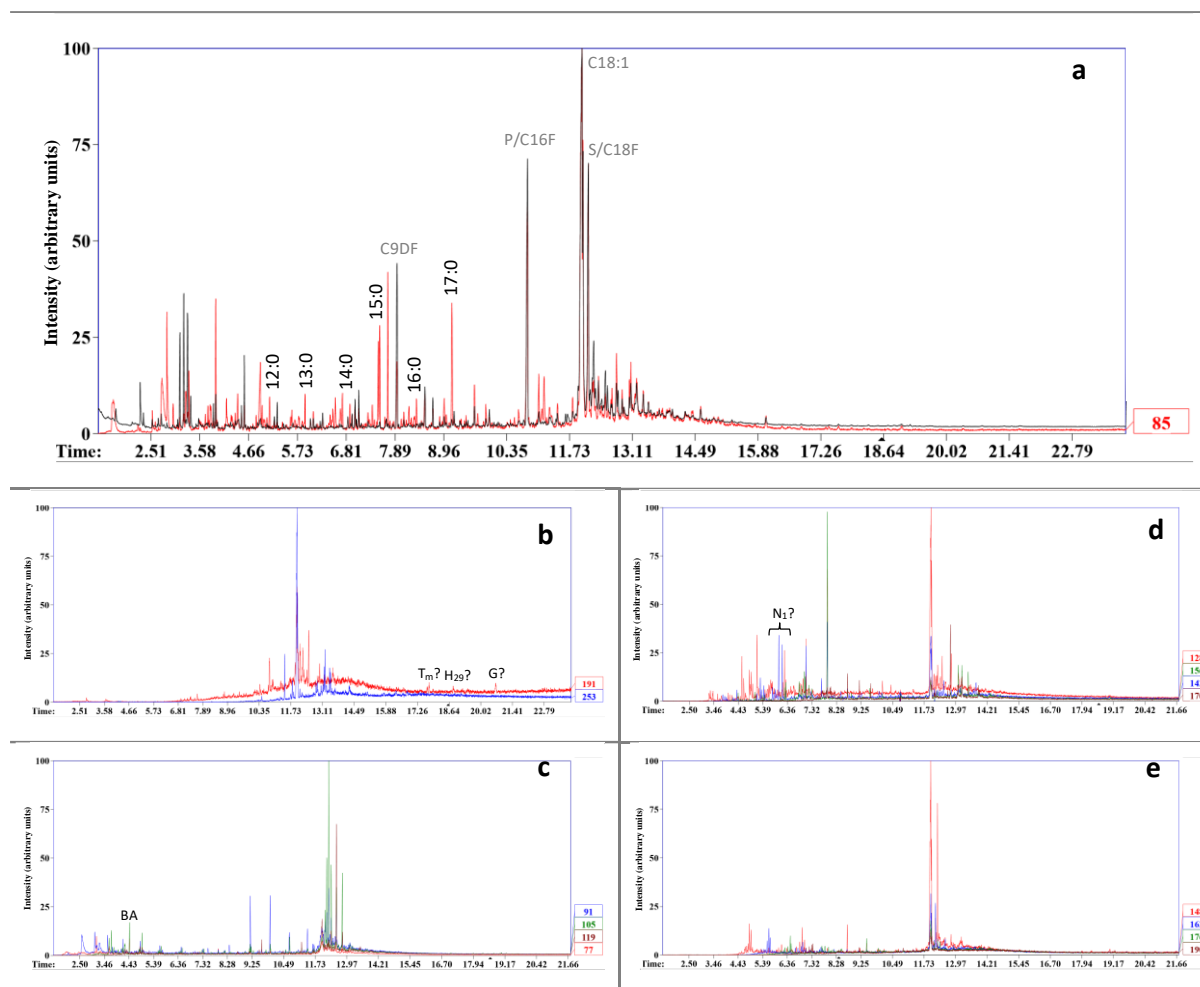


Figure 5: Mass chromatograms of sample KT-I, a) TIC (in black) and alkanes (m/z 85), b) tricyclic terpanes and hopanoids (m/z 191 in red) and C-ring monoaromatic steroids (m/z 253 in blue), c) alkylbenzenes (m/z 91, 77, 105, 119), d) alkylnaphthalenes (m/z 128, 142, 156, 170) and e) alkylbenzenes (m/z 148, 162, 176, 190) in Py-TMAH-GC/MS.

Although the focus of the analysis is the tracking of the TLA features it is important to note that the main compounds present in the mass chromatogram of sample KT-I are fatty acids (determined by the m/z 74) identified in Fig. 10. Clearly, the use of TMAH for derivatisation was the easiest means for exhaustively characterizing their presence. However, the predominance of the methyl esters may have obscured minor amounts of asphaltic components pushed below the detection limit. Nevertheless, as shown below, direct Py-GC_xGC/MS analysis without TMAH still confirmed the absence of these compounds in KT-I.

In fact for the KT-I, KT and RP samples, saturated short and long-chain fatty acids (F) from C3F up to C27F and unsaturated C18 fatty acids could be observed along with short-chain diacids (DF) down to C4DF (Fig. 6). The highest peak belongs to the C18 mono-unsaturated fatty acid, followed by the saturated fatty acids C16 and C18, palmitic and stearic acid respectively. Although cooked at high temperature with lead compounds, these samples contain high amounts of oxidised C18 fatty acids, short fatty acids chains and glycerol compounds (gly), but a low amount of diacids when compared with naturally aged paint samples [21].

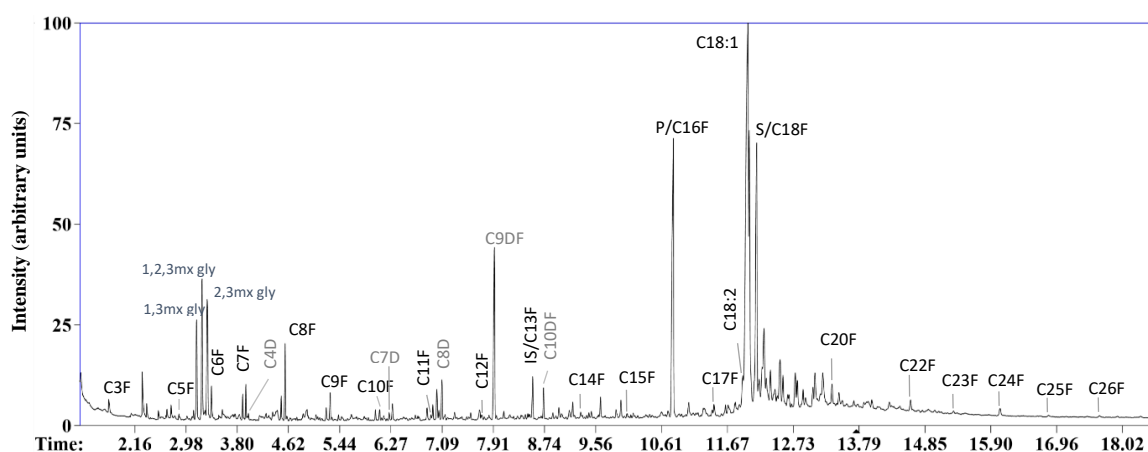


Figure 6: Total ion chromatogram of the KT-I sample derivatized with TMAH. “F” stands for fatty acids while “DF” for diacids, and “mx gly” identifies the glycerol derivatives.

3.2 Py-GCxGC/MS

3.2.1 Asphalt features in the TLA reference sample

Complementary to Py-TMAH-GC/MS, the same samples were analysed by Py-GCxGC/MS to determine whether this technique with its higher resolution and lower limit of detection, could help in the identification of asphalt in paint samples where the asphalt may be diluted by the paint production method. The reference sample of TLA was analysed in duplicate by direct Py-GCxGC/MS without derivatization since the targeted compounds detected above as potential markers for the TLA sample are not affected by methylation.

The series of markers and biomarkers previously observed with Py-TMAH-GC/MS were confirmed and refined thanks to the increased resolution provided by the bidimensional chromatographic separation. Figure 7 reports the resulting total ion chromatogram obtained after pyrolysis at 600°C of the TLA reference samples. Both the total ion chromatogram and the extracted ion chromatograms of the compounds of interest, (as specified above, see Experimental) were used for the characterization of components in the reference sample.

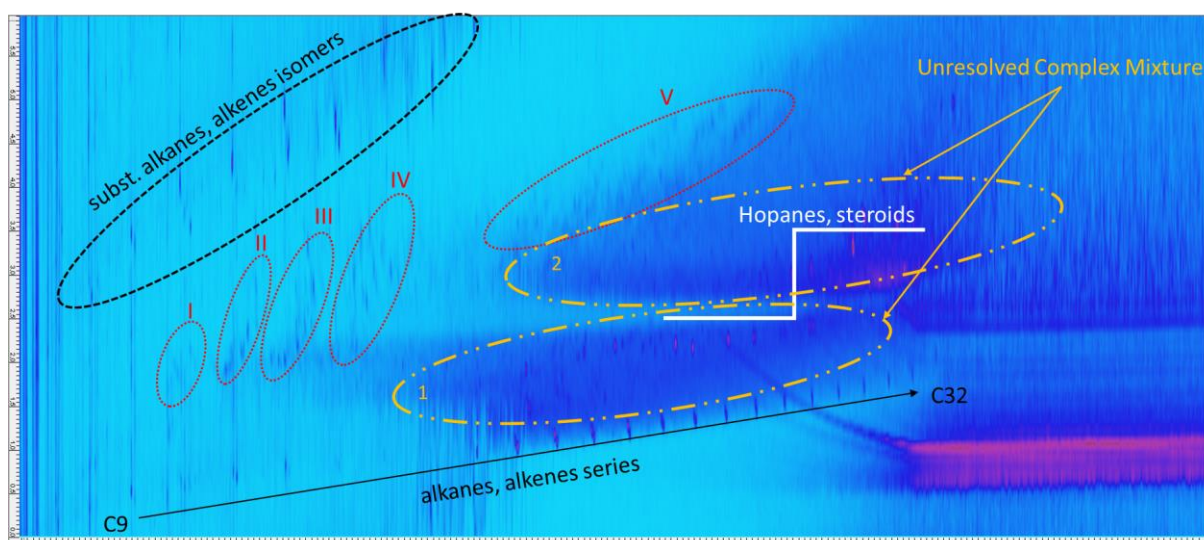


Figure 7: Total ion chromatogram of the TLA obtained by Py-GCxGC/MS for a reference sample of 39 μg (see experimental part for details). Families of compounds are circled in black, red and yellow.

Three large areas of unresolved complex mixtures spanning from $^1t_R = 40$ min to 90 min can be differentiated from the regular bleeding of the columns in the Py-GCxGC/MS chromatogram. This is responsible for the high level of background noise observed during the Py-TMAH-GC/MS experiments. Although the identification of the associated components is difficult, it can be stated that in area 1 circled in yellow (Fig. 7) the peak distributions are attributable to hydrocarbons with a classical series of fragments at m/z 41, 43, 55, 57, 69, 71, 83, 85 etc. while in area 2 there are different fragmentation patterns with unclear significance. The 3D-view (Fig. S1, SM) of the Py-GCxGC/MS chromatogram confirmed that most of the signal from the pyrolysis of the TLA reference sample lies in a series of linear hydrocarbons consisting of substituted alkanes or alkanes isomers; of hopanes structures; and of the unresolved complex mixture.

The families of compounds observed in Figure 7 outlined in black, red and yellow, will be the point of interest for tracking asphalt features in the reconstruction samples and are briefly detailed below and compiled in Table S1 (SM). They consist mainly of a series of alkanes/alkenes, a series of branched alkanes and isomers of alkenes, a series of hopanoid homologs and groups of compounds (I to V outlined in red). As will be seen below, the evolution of intensity of these compounds compared with the relative intensities of compounds from the unresolved complex mixture can be considered in the following samples. It is important to note that among the components detected during pyrolysis, few sulphur containing compounds were present. Some sulphur compounds were evident as methyl-substituted benzothiophenes. However no derivatives were observed of thiolanes, thianes, alkyl thiophenes, isoprenoid or steroid sulphides, which would be expected from asphalt [19]. Extracted ion procedures were applied in an effort to select the relevant m/z fragments in the mass spectra, basically base peaks, of these compounds [19,34].

A series of alkanes and alkenes ranging from C9 (nonene) to C32 (dotriacontane) were observed as a predominant feature in the TIC (Fig. 7). Their distribution showed disparities, while almost all the alkane homologs incremented in carbon number were detected, some of the associated alkenes were missing in the series, in particular for carbon chains exceeding C24 for which no alkene homologs were clearly separated from their alkane homologs or even present (Table S1 in SM). In addition, a gap was present in the alkanes/alkenes series between the C14 and C18 homologs. In addition to this series of

linear hydrocarbons, additional peaks assigned to substituted alkanes or positional isomers of alkenes and shifted in time in the second dimension ($t_R = 3-6$ s in Figure 7) are visible in the chromatogram.

Among the expected compounds of interest from the alkane series, neither phytane (m/z 282) nor pristane (m/z 268), were detected during pyrolysis of the TLA reference samples. This result corroborates well the data obtained with Py-TMAH-GC/MS.

Regarding the presence of fatty acids, only the n-hexadecanoic acid methyl ester was detected in both TLA reference samples in low quantity under the chosen conditions of analysis without the use of TMAH. However, traces of myristic acid methyl ester (C14) and stearic acid methyl ester (C18) could be observed in one of the TLA reference samples.

Among the expected biomarkers, a series of hopanes and monoaromatic steroids were observed (Table S1 in SM). An extracted ion procedure, selecting the m/z fragments at m/z 191 and 253, present as base peak in the mass spectra, was applied to characterize the hopanes and steroids. Both series of these compounds are eluting among the unresolved complex mixture (in area 2 circled in yellow, Fig. 7). The hopane series can be differentiated into hopane and norhopane structures. Noteworthy, no steranes, which could be expected as markers in an asphalt [12], were characterized during pyrolysis of the TLA reference sample.

The extracted ion procedure at m/z 91 revealed the presence of single aromatics: toluene and isomers of dimethyl-benzene. Extended search at m/z 105, 119 revealed the presence of substituted tri- and tetramethyl-benzene homologues. No trace of benzoic acid was detected however this can be explained by the lack of methylation which is needed for its efficient detection. In contrast to the findings with Py-TMAH-GC/MS, structures with a base peak at m/z 128 and assigned to naphthalene and 1-methylene-1H-indene, respectively, were detected using Py-GCxGC/MS (Table S1 in SM). Alkylbenzenes, akylnaphthalenes, and alkylbenzothiophenes previously detected with Py-TMAH-GC/MS were revealed in four groups of compounds, identified as I, II, III and IV in Figure 7. The first group I consists mainly of methyl-substituted benzenes, the previously mentioned naphthalene and substituted indene structures. Group II encompasses dimethyl substituted indene structures and methylated naphthalenes. Group III includes trimethyl substituted indene structures, dimethyl naphthalene isomers, and dimethylbenzothiophenes as well as their dibenzothiophene homologs. Group IV encompasses the higher homologs with trimethylated naphthalenes and trimethylated benzothiophenes. An additional group, identified as group V in Figure 7, consisted of a series of polycyclic aromatic hydrocarbons including phenanthrene to pyrene substituted structures.

3.2.2 Asphalt features in the Reconstructions

Having established a full chemical fingerprint of the TLA reference sample using the findings above, sample KT-I from heating asphalt with lead-treated drying oil was investigated to determine any changes resulting during the manufacture of W&N's bitumen brown oil paint (Table S1 in SM).

3.2.2.1 TLA features in sample KT-I

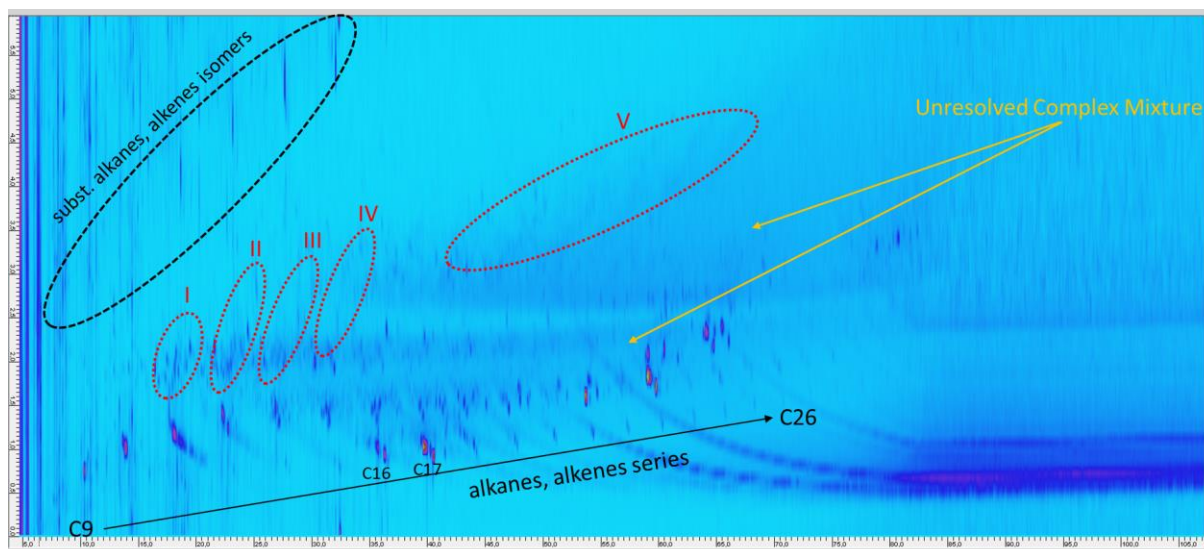


Figure 8: Total ion chromatogram of the KT-I sample obtained by Py-GCxGC/MS of 53 μg of sample. Families of compounds are circled in black, red and yellow.

Compared to the TLA reference sample, the unresolved complex mixture is significantly attenuated in the total ion current chromatogram from sample KT-I (Fig. 8). The 3D-view of the Py-GCxGC/MS chromatogram confirmed this diminution in relative intensity when compared to the overall intensities of peaks assigned to the targeted compounds (Fig. S2 in SM). In KT-I most of the signal is taken up by components from the addition of drying oil (see below). However patterns from the TLA reference sample were still detectable, specifically the series of linear hydrocarbons, substituted alkanes or alkanes isomers. Families of compounds which remain in KT-I are briefly detailed below and compiled in SM Table S1.

A notable change in the series of alkanes and alkenes from C9 to C26 (longer than those detected by Py-TMAH-GC/MS which were limited to the C12-C17 homologs) was observed in KT-I compared to the TLA reference sample, in particular, an abnormally intense pattern of peaks assigned to 1-n-heptadecene/n-heptadecane structures was detected in the middle of the series around $^1t_{\text{R}}=40$ min. This group of four components was attributed to heptadiene $^1t_{\text{R}}=39.4$ min, isomer of 1-n-heptadecene, $^1t_{\text{R}}=39.7$ min, 1-n-heptadecene $^1t_{\text{R}}=40.2$ min and heptadecane $^1t_{\text{R}}=40.5$ min, respectively. A similar pattern, however with comparatively lower intensities, was observed for the C16 homologs, with strong peaks associated to the 1-n-hexadiene and hexadiene, and with low intensity for the n-hexadecane. Interestingly the highest intensities of the C16 and C17 alkanes/alkenes homologs seen in KT-I had not been observed in the TLA reference sample since these compounds were missing. The presence of C16-17 hydrocarbons in the KT-I sample could result from the scission of alkyl chains of fatty acids during the pyrolysis process and are likely attributable to the addition of drying oil.

In the KT-I sample, additional peaks assigned to substituted alkanes or positional isomers of the alkenes and shifted in time in the second dimension ($^2t_{\text{R}}=2.5\text{-}6$ s in Figure S2 in SM) appeared in the chromatogram which was similar to the TLA reference.

Among the expected biomarkers of asphalt, a series of hopanes and monoaromatic steroids were observed in the TLA reference during Py-TMAH-GC/MS analysis (Table 2). Application of the extracted ion procedure to the KT-I sample, selecting the m/z fragments at m/z 191 and 253 for the characterization of hopanes and steroids did not reveal their presence. Similarly, an extracted ion

chromatogram (EIC) at m/z 230 for the detection of pyrene or terphenyls in the KT-I sample did not find these materials whereas they were detected in the TLA reference sample. Clearly, these compounds were eliminated in the first step of the reconstruction of the bitumen brown oil paint.

Extracting the fragments at $m/z=91$ showed more benzene and naphthalene homologs than had been observed in the TLA reference sample. At the beginning of the chromatogram for KT-I, for $^1t_R < 17$ min, these compounds correspond to unsaturated alkylbenzenes and dehydrogenated naphthalene (Table S1 in SM). Moreover new structures are observed, in particular a series of alkylbenzenes expanding to the undecyl-benzene $C_{17}H_{28}$, which could be related to radical condensation products and be explained by the addition of drying oil.

Application of the extracted ion procedure at the fragments m/z 119 in sample KT-I did not reveal the presence of group I components, tetramethyl-, benzene, observed in the TLA reference sample. Instead, EIC at m/z 119 showed mainly aromatic structures built around a substituted benzene ring (Table S1 in SM).

Similarly, benzothiophene based structures belonging to group I and group II were absent. In contrast, the 1H-Indene, 1-methylene-, 2-methylindene, 1H-Indene, dimethyl-, naphthalene structure were still present. The same applies for the dimethyl, indene (group II) which are still detected, while benzothiophene structures are absent.

However, EICs at m/z 142 for the KT-I sample showed that most of the compounds found during pyrolysis of the TLA reference sample, such as the benzocycloheptatriene structures, 1-H-indene structures, 1- or 2-methylnaphthalene (group II) were still present. Overall, group II provided almost the same number of components as those detected in the reference sample of TLA.

As observed for the benzothiophene based structure of group I, none of the dimethyl, benzothiophenes (EICs at m/z 162) were detected as representative compounds of group III. The same does not apply for most of the dimethyl, naphthalene homologs still prevailing in group III as well as the trimethyl, indene-based structures.

In a similar way, for group IV, only the substituted naphthalene (trimethyl-) remained while the main benzothiophene substituted homologs were missing.

In general the presence of markers of asphalt are noticeably decreasing in the two last groups, IV and V, compared to the TLA reference. The most significant finding is that all sulphur containing compounds which had been observed in the TLA reference sample are absent in the KT-I sample, (which was taken very early on in the preparation of the bitumen brown oil paint reconstruction).

Whereas a significant number of compounds characterized during Py-GCxGC/MS analysis of the TLA reference sample were not detected in the KT-I sample, some compounds within the different groups defined earlier were still detected. However, these compounds are mixed with new class of components introduced by the materials used in the reconstruction of bitumen paint. In particular, alkyl acids C5-C8, propenyl ester of alkyl acids C11-C21, and carbonylated compounds were eluted in $^2t_R= 1-2.5$ s (Fig. 8).

Dilution of the asphalt in the oil paint mixture or chemical breakdown of the whole asphalt structure were proposed as possible explanations for the results of the Py-TMAH-GC/MS analyses. The Py-GCxGC/MS analyses results were led to similar findings with greater emphasis on the second explanation, that a chemical breakdown of the asphalt structure was occurring: an assumption supported by the disappearance of the benzothiophene homologs.

To understand the effect of temperature (during paint manufacturing) an additional TLA sample heated to 318°C was analysed with Py-GCxGC/MS (see Table S1 in SM). Contrarily to the results observed with the TLA reference sample, the heated TLA had predominantly alkyl homologs C14-C18 which could likely be attributed to the thermal degradation of alkyl bridges of the asphaltene structure in the asphalt sample. However, the marker compounds (hopanes, monoaromatic steroids and groups I-V) were still observed in the heated TLA sample with no noticeable change in their distribution except an increased number of aromatic homologs in group IV-V. Therefore, the temperature of cooking does not appear to cause the disappearance of sulphur compounds, or induce significant differences in the compounds distribution detectable by Py-GCxGC/MS.

4. Conclusion

In summary, the analysis of the TLA reference sample with both techniques showed specific markers and biomarkers that could be used to identify the presence of the original TLA in the reconstruction samples:

- An homologous series of alkanes and alkenes, with Py-GCxGC/MS identifying additional peaks assigned to substituted alkanes or positional isomers of alkenes;
- Monoaromatic steroids;
- A series of hopanoid homologs (which can be differentiated into hopane and norhopane structures);
- The pentacyclic triterpenoid gammacerane;
- Compounds issued from the aromatic sheet structure of asphaltene such as the alkylbenzenes, alkyl naphthalenes and alkylbenzothiophenes, further characterized with Py-GCxGC/MS and reported as five groups of compounds:
 - Group I: mainly methyl-substituted benzenes, the previous naphthalene and substituted indene structures.
 - Group II: dimethyl substituted indene structures and methylated naphthalenes.
 - Group III: trimethyl substituted indene structures, dimethyl naphthalene isomers, and dimethylbenzothiophenes as well as their dibenzothiophene homologs.
 - Group IV: higher homologs with trimethylated naphthalenes and trimethylated benzothiophenes.
 - Group V: series of polycyclic aromatic hydrocarbons including phenanthrene to pyrene substituted structures.

Interestingly, few sulphur containing compounds were present, such as, methyl-substituted benzothiophenes, and no derivatives of thiolanes, thianes, alkyl thiophenes, isoprenoid or steroid sulphides were observed.

The unresolved complex mixture is more easily discerned with Py-GCxGC/MS in the TLA reference sample, although it remains visible throughout samples from the reconstruction this mixture became noticeably attenuated at each stage with a marked diminution in relative intensity. Given the mineral content in the TLA sample, it is possible that large complex organo-metallic compounds play a role in this unresolved complex mixture. However, it is important to note that supplementary analysis of other sources of asphalt or bitumen (not discussed here) do not show this unresolved complex mixture and therefore this should not be considered a “feature” to track asphalts in oil paintings.

The main conclusion from this study is that with both analytical techniques, the main TLA markers have already disappeared in the first step of the reconstruction (sample KT-I), and those remaining, such as the series of alkanes, are insufficiently characteristic to make an unequivocal attribution for asphalt. This finding is extremely important for any conclusions based on analyses using Py-TMAH-GC/MS or Py-GCxGC/MS of 19th century paintings suffering from film-forming defects thought to have been associated with the use of asphalt.

The use of the highly sensitive technique of Py-GCxGC/MS in this study illustrates that the difficulty in identifying asphalt markers in historical paint is not simply due to its dilution during paint production, rather these findings indicate that in the case of Trinidad Lake asphalt at least, the original asphalt markers disappear during heating and processing in drying oil.

In this case it is thought that the asphalt is possibly undergoing reduction due to the loss of sulphur bridges, possibly favoured in the presence of lead, which results in the chemical breakdown of the asphalt and the disappearance of thiophenes visible in the original material. Considering the TLA processing and ingredients added up to the first step of the reconstruction, the interaction with the drying oil and respective lead driers are dominant factors for the absence of asphalt features. Further chemical study on the effects of lead oxide on polysulphides and bound sulpherised lipids would be relevant here to better understand this process.

Acknowledgements

CORES Ph.D. programme PD/00253/2012 and LAQV-Requimte UIDB/50006/2020 and UIDP/50006/2020. Special thanks to Dr. Klaas Jan van den Berg for facilitating access to the Py-TMAH-GC/MS equipment at the RCE (Cultural Heritage Agency of the Netherlands) and to Henk van Keulen for performing the Py-TMAH-GC/MS analyses. The authors would also like to acknowledge the help of Davy Safrano who run the Py-GCxGC/MS analysis at the CRCC (Centre de Recherche sur la Conservation des Collections) in Paris.

References

- [1] L.S. Van der Loeff, K. Groen, The Restoration and Technical Examination of Gerard Dou's The Young Mother in the Mauritshuis, in: J. Bridgland (Ed.), ICOM-CC 10th Trienn. Meet. Washington, DC, USA, 22–27 August 1993, ICOM Committee for Conservation, Washington, 1993: pp. 98–103.
- [2] C. Bothe, Asphalt, in: B.H. Berrie (Ed.), Artist. Pigment. A Handb. Their Hist. Charact., Volume 4, Archetype Publications Ltd., London, 2007: pp. 111–149.
- [3] L. Carlyle, A. Southall, No Short Mechanical Road to Fame: The Implications of Certain Artists' Materials for the Durability of British Painting: 1770-1840, in: R. Hamlyn (Ed.), Robert Vernon's Gift. Br. Art Nation 1847, Tate Gallery Publications, Millbank, London, 1993: pp. 21–26.
- [4] L. Carlyle, The Artist's Assistant Oil Painting Instruction Manuals and Handbooks in Britain 1800-1900 With Reference to Selected Eighteenth-century Sources, Archetype Publications Ltd., London, 2001.

- [5] G.M. Languri, Molecular studies of Asphalt, Mummy and Kassel earth pigments, their characterisation, identification and effect on the drying of traditional oil paint, University of Amsterdam, 2004.
- [6] K. Groen, A seventeenth-century use of bituminous paint, *Bull. Hamilt. Kerr Inst.* 2 (1994) 84.
- [7] R. White, Brown and Black Organic Glazes, *Pigments and Paints, Natl. Gall. Tech. Bull.* 10 (1986) 58–71.
- [8] A. Nissenbaum, Dead Sea asphalts - Historical aspects, *Am. Assoc. Pet. Geol. Bull.* 62 (1978) 837–844.
- [9] R. Marques, L. Carlyle, L. De Viguerie, I. Pombo Cardoso, J.J. Boon, Winsor & Newton's 19th-century bitumen brown oil paint. Part I: a critical analysis of W&N production records, in: D. Oltrogge, J.H. Townsend, A. Haack-Christensen, M. Stols-Witlox (Eds.), *Reflecting Reconstr. Role Sources Performative Methods Art Technol. Stud. Proc. Eighth Symp. ICOM-CC Work. Gr. ATSR, Held Col. Inst. Conserv. Sci.* 26-27 Sept. 2019., ICOM-CC, 2022: pp. 49–64.
- [10] R. Marques, L. Carlyle, L. De Viguerie, I. Pombo Cardoso, J.J. Boon, Winsor & Newton's 19th-century bitumen brown oil paint. Part II: the reconstruction, in: D. Oltrogge, J.H. Townsend, A. Haack-Christensen, M. Stols-Witlox (Eds.), *Reflecting Reconstr. Role Sources Performative Methods Art Technol. Stud. Proc. Eighth Symp. ICOM-CC Work. Gr. ATSR, Held Col. Inst. Conserv. Sci.* 26-27 Sept. 2019., ICOM-CC, 2022: pp. 65–76.
- [11] R. Aydemir, M. Eren, H. Askun, A.E. Özbey, M. Orbay, Bitumen paints, an old story with new approach, part-1, solvent based paints, *Prog. Org. Coatings.* 76 (2013) 966–971. <https://doi.org/10.1016/j.porgcoat.2012.10.016>.
- [12] K.E. Peters, C.C. Walters, J.M. Moldowan, *The Biomarker Guide. Volume 1. Biomarkers and Isotopes in the Environment and Human History.*, Second Edi, Cambridge University Press, Cambridge, United Kingdom, 2005. [https://doi.org/10.1016/0146-6380\(93\)90028-a](https://doi.org/10.1016/0146-6380(93)90028-a).
- [13] T.F. Yen, Asphaltic Materials, in: H.F. Mark (Ed.), *Encycl. Polym. Sci. Eng.*, 2nd ed., Wiley-Interscience, New York, 1990: pp. 1–10.
- [14] J. Claine Petersen, Chemical Composition of Asphalt as Related to Asphalt Durability: State of the Art, *Transp. Res. Rec.* (1984) 13–30.
- [15] X. Yu, N.A. Burnham, M. Tao, Surface microstructure of bitumen characterized by atomic force microscopy, Elsevier B.V., 2015. <https://doi.org/10.1016/j.cis.2015.01.003>.
- [16] O.C. Mullins, H. Sabbah, J. Eyssautier, A.E. Pomerantz, L. Barré, A.B. Andrews, Y. Ruiz-Morales, F. Mostowfi, R. McFarlane, L. Goual, R. Lepkowicz, T. Cooper, J. Orbulescu, R.M. Leblanc, J. Edwards, R.N. Zare, *Advances in Asphaltene Science and the Yen-Mullins Model, Energy and Fuels.* 26 (2012) 3986–4003. <https://doi.org/10.1021/ef300185p>.
- [17] J.S. Mills, R. White, *The Organic Chemistry of Museum Objects*, 1st editio, Butterworth, London, 1987.
- [18] G.M. Languri, J. van der Horst, J.J. Boon, Characterisation of a unique “asphalt” sample from the early 19th century Hafkenscheid painting materials collection by analytical pyrolysis MS and GC/MS, *J. Anal. Appl. Pyrolysis.* 63 (2002) 171–196. [https://doi.org/10.1016/S0165-2370\(01\)00153-X](https://doi.org/10.1016/S0165-2370(01)00153-X).
- [19] J.S. Sinninghe Damste, J.W. De Leeuw, Analysis, structure and geochemical significance of organically-bound sulphur in the geosphere: State of the art and future research, *Org. Geochem.* 16 (1990) 1077–1101. <https://doi.org/https://doi.org/10.1016/0146->

6380(90)90145-P.

- [20] M.E.L. Kohnen, Sulphurised Lipids in Sediments: The key to reconstruct paleobiochemicals and their origin, Delft Technical University, Delft (NL), 1991.
- [21] J.D.J. van den Berg, Analytical chemical studies on traditional linseed oil paints, University of Amsterdam, 2002.
- [22] I. Bonaduce, A. Andreotti, Py-GC/MS of Organic Paint Binders, in: *Org. Mass Spectrom. Art Archaeol.*, 2009: pp. 303–326. <https://doi.org/10.1002/9780470741917.ch11>.
- [23] B. Han, G. Daheur, M. Sablier, Py-GCxGC/MS in cultural heritage studies: An illustration through analytical characterization of traditional East Asian handmade papers, *J. Anal. Appl. Pyrolysis*. 122 (2016) 458–467. <https://doi.org/https://doi.org/10.1016/j.jaap.2016.10.018>.
- [24] B. Han, J. Niang, H. Rao, N. Lyu, H. Oda, S. Sakamoto, Y. Yang, M. Sablier, Paper fragments from the Tibetan Samye Monastery: Clues for an unusual sizing recipe implying wheat starch and milk in early Tibetan papermaking, *J. Archaeol. Sci. Reports*. 36 (2021) 102793. <https://doi.org/https://doi.org/10.1016/j.jasrep.2021.102793>.
- [25] B. Han, X. Fan, Y. Chen, J. Gao, M. Sablier, The lacquer crafting of Ba state: Insights from a Warring States lacquer scabbard excavated from Lijiaba site (Chongqing, southwest China), *J. Archaeol. Sci. Reports*. 42 (2022) 103416. <https://doi.org/https://doi.org/10.1016/j.jasrep.2022.103416>.
- [26] P.Q. Tranchida, F.A. Franchina, P. Dugo, L. Mondello, Comprehensive two-dimensional gas chromatography-mass spectrometry: Recent evolution and current trends, *Mass Spectrom. Rev.* 35 (2016) 524–534. <https://doi.org/https://doi.org/10.1002/mas.21443>.
- [27] R. Charles, F. Grimaldi, Trinidad Lake Asphalt in Pavement Performance, *West Indian J. Eng.* 18 (1996) 29–40.
- [28] H. Pasco, L. Carlyle, M. Faustini, H. Glanville, C. Sanchez, P. Walter, L. de Viguerie, Investigating Nineteenth Century Gel Mediums: From Historical Recipes to Model Systems, *Stud. Conserv.* (2022). <https://doi.org/10.1080/00393630.2022.2031530>.
- [29] G.P. Kayukova, B. V. Uspensky, I.M. Abdrafikova, R.Z. Musin, Characteristic features of the hydrocarbon composition of Spiridonovskoe (Tatarstan) and Pitch Lake (Trinidad and Tobago) asphaltites, *Pet. Chem.* 56 (2016) 572–579. <https://doi.org/10.1134/S0965544116070082>.
- [30] E.A. Subroto, R. Alexander, R.I. Kagi, 30-Norhopanes: their occurrence in sediments and crude oils, *Chem. Geol.* 93 (1991) 179–192. [https://doi.org/10.1016/0009-2541\(91\)90071-X](https://doi.org/10.1016/0009-2541(91)90071-X).
- [31] H.P. Nytoft, G. Kildahl-Andersen, T. Šolević Knudsen, K. Stojanović, F. Rise, Compound “J” in Late Cretaceous/Tertiary terrigenous oils revisited: Structure elucidation of a rearranged oleanane coeluting on GC with 18 β (H)-oleanane, *Org. Geochem.* 77 (2014) 89–95. <https://doi.org/10.1016/j.orggeochem.2014.09.010>.
- [32] K.E. Peters, C.C. Walters, J.M. Moldowan, *The Biomarker Guide. Volume 2. Biomarkers and Isotopes in Petroleum Exploration and Earth History*, Second Ed, Cambridge University Press, Cambridge, United Kingdom, 2005. <https://doi.org/10.1017/cbo9781107326040>.
- [33] I. Bonaduce, L. Carlyle, M.P. Colombini, C. Duce, C. Ferrari, E. Ribechini, P. Selleri, M.R. Tine, A multi-analytical approach to studying binding media in oil paintings: Characterisation of differently pre-treated linseed oil by DE-MS, TG and GC/MS, *J. Therm. Anal. Calorim.* 107 (2012) 1055–1066. <https://doi.org/10.1007/s10973-011-1586-6>.
- [34] M.E. Machado, F. Cappelli Fontanive, J.V. de Oliveira, E.B. Caramão, C. Alcaraz Zini,

Identification of organic sulfur compounds in coal bitumen obtained by different extraction techniques using comprehensive two-dimensional gas chromatography coupled to time-of-flight mass spectrometric detection, *Anal. Bioanal. Chem.* 401 (2011) 2433–2444. <https://doi.org/10.1007/s00216-011-5171-4>.

Funding

This work was financially supported by the Portuguese Foundation for Science and Technology (FCT-MCTES) through PhD grant PD/BD/135058/2017 (Raquel Marques, PhD working title “Craquelure Anglaise: The development of film-formation defects in European 19th century oil paintings leading to paint failure and a loss of image integrity”). This work was supported by the Associate Laboratory for Green Chemistry - LAQV which is financed by national funds from FCT/MCTES (UIDB/50006/2020 and UIDP/50006/2020).

Supplementary Material

3D-views of the GCxGC/MS chromatograms:

The reconstructed 3D-view of the bidimensional GCxGC chromatograms can be used as a quick mean to estimate the relative intensities of peaks pertaining to each component of the sample during the Py-GCxGC/MS analysis. To illustrate this, comparison of the 3D-views of the TLA reference sample (Figure S1) and of the KT-1 sample (Figure S2) show a diminution of the relative intensity of peaks associated to the complex unresolved mixture compare to the other components of the TLA (alkanes/alkenes, cyclic alkanes, groups I-V) with an intensity scale varying from the $10 \cdot 10^6$ to $80 \cdot 10^6$ range in the second dimension (Column II). Please refer to the text for further details.

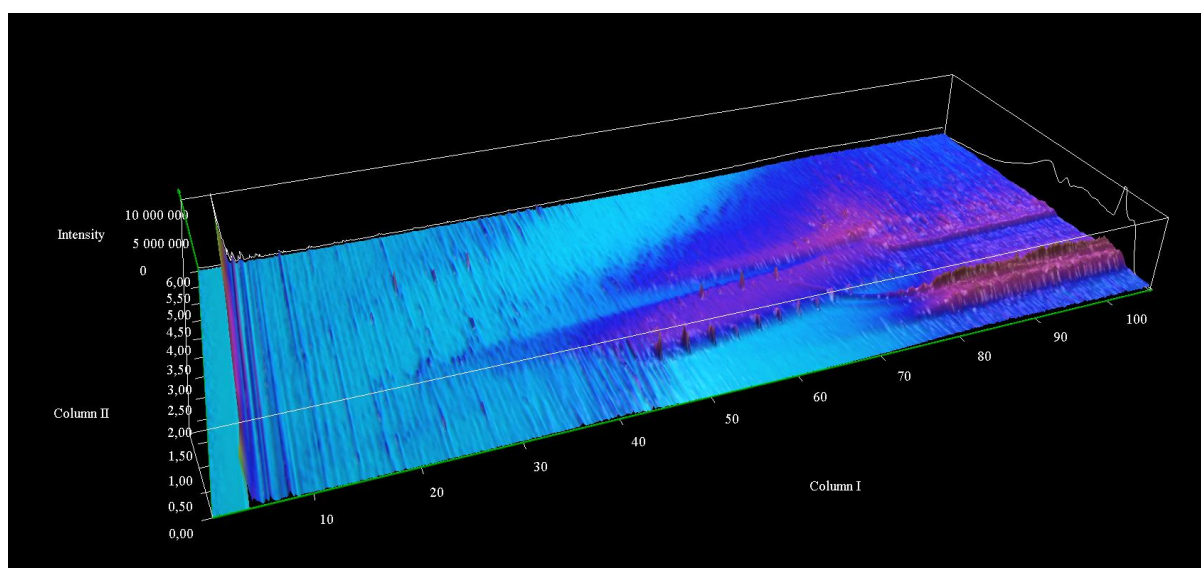


Figure S1. 3D view of total ion chromatogram of the TLA reference sample obtained by Py-GCxGC/MS for a sample of 39 μg (see experimental part for details).

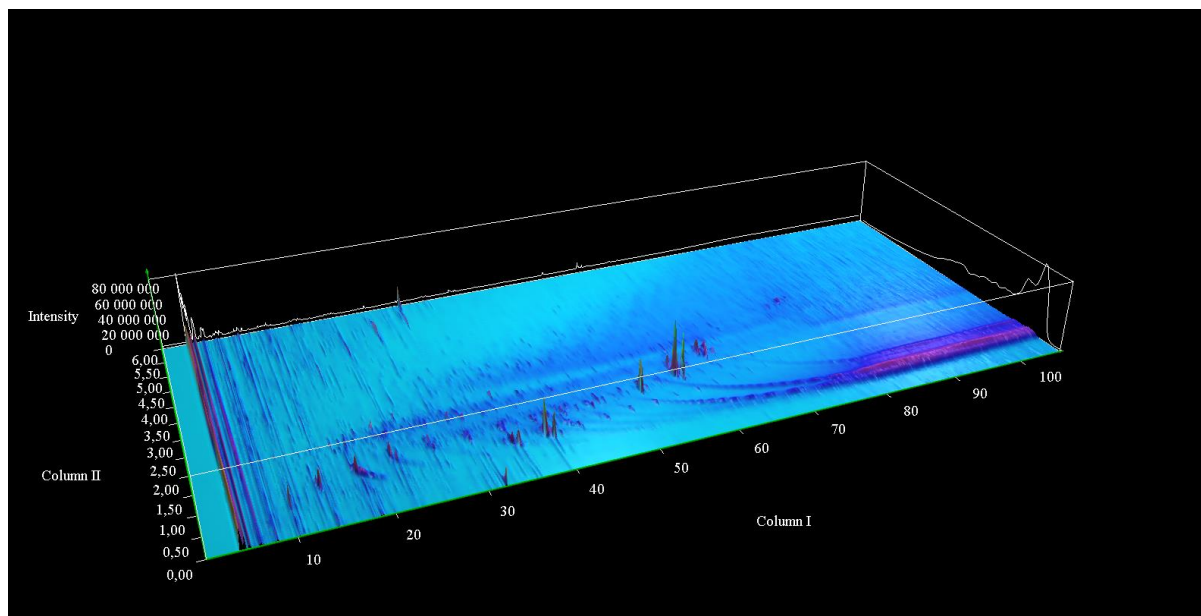


Figure S2. 3D view of total ion chromatogram of the KT-I sample obtained by Py-GCxGC/MS for a sample of 53 μg (see experimental part for details).

Table S1. Assignment of compounds detected by Py-GCxGC/MS in the investigated TLA reference sample and the three steps of the reconstruction recipes, R2-1, KT-2 and RP2, with retention time in the first and second dimension (1tr, 2tr), main fragment ions, expected molecular weights, assigned formula, most likely attribution of the products and their observed presence or absence in the resulting chromatograms.

Compounds	¹ t _r (min)	² t _r (s)	Fragment ions (in decreasing order of intensity)	MW	Formula	Assignment ^a	TLA ^b	Heated TLA ^b	KT-1 ^b	KT ^b	RP ^b
Alkanes, Alkenes											
	8,1	0,1	56,43,55,41,70	126	C9H18	1-Nonene	x	x	x	x	-
	10,8	0,3	41,56,55,70,43	140	C10H20	n-1-Decene	x	x	x	x	-
	11	0,3	57,43,71,79,85	142	C10H22	n-decane	-	-	x	-	-
	14,4	0,5	41,43,56,55,70	154	C11H22	n-1-Undecene	x	x	-	x	x
	14,7	0,4	57,43,71,41,85	156	C11H24	n-Undecane	x	x	x	-	-
	18,7	0,6	41,43,55,70,56	168	C12H24	n-Dodecene	x	-	x	x	x
	19	0,55	57,43,71,41,85	170	C12H26	n-Dodecane	x	-	x	-	-
	23,2	0,7	56,55,57,69,41	182	C13H26	n-1-Tridecene	x	x	x	x	x
	23,5	0,65	57,43,71,41,85	184	C13H28	n-Tridecane	x	x	-	-	x
	27,7	0,8	55,41,70,57,56	196	C14H28	n-1-Tetradecene	x	x	x	x	x
	28	0,75	57,43,71,41,85	198	C14H30	trace tetradecane	x	x	x	-	-
	32,03	0,85	55,43,41,57,83	210	C15H30	n-1-pentadecene	-	x	-	-	x
	32,3	0,75	57,43,71,41,85	212	C15H32	Pentadecane	-	x	x	-	x
	35,7	1	55,41,67,81,82	222	C16H30	1,15-Hexadecadiene	-	-	x	-	-
	35,9	0,9	55,69,43,56,83	224	C16H32	isomer of hexadecene	-	x	x	-	-
	36,3	0,9	55,43,57,41,83	224	C16H32	n-1-Hexadecene	-	x	x	-	x
	36,5	0,85	57,43,71,85,41	226	C16H34	Hexadecane	-	x	x	-	-
	39,4	1,1	55,41,67,81,82	236	C17H32	heptadiene	-	x	x	-	-
	39,7	1	55,69,41,43,83	238	C17H34	isomer of heptadecene	-	x	x	x	x
	39,9	1	55,41,69,43,57	238	C17H34	8-Heptadecene	-	-	-	x	-
	40,2	0,2	55,57,43,41,69	210	C15H30	n-1-pentadecene	x	-	x	x	-

40,5	0,9	57,71,43,41,85	240	C17H36	heptadecane	-	X	x	x	-
41,5	0,95	56,57,69,70,43	266	C19H38	1-hexadecene, 5 methyl	-	X	x	-	-
43,23	1,1	55,81,41,67,82	250	C18H34	isomer of octadecene	-	-	-	x	x
43,5	1,1	67,55,81,41,82	250	C18H34	isomer of octadecene	-	-	-	x	-
44	1,05	55,57,43,41,69	252	C18H36	1-n-octadecene	-	X	x	x	x
44,2	0,9	57,43,71,85,41	254	C18H38	Octadecane	x	X	x	x	-
47,5	1,05	43,57,55,97,83	266	C19H38	1-n-nonadecene	x	X	x	x	x
47,7	1	57,43,71,85,41	268	C19H40	nonadecane	x	X	x	x	-
50,9	1,15	43,55,57,83,69	280	C20H40	1-n-eicosene	x	X	x	x	x
51,1	1,05	57,71,43,85,41	282	C20H42	Eicosane	x	X	x	x	-
54,1	1,2	43,55,57,83,41	294	C21H42	n-1-Heneicosene	x	X	x	x	-
54,3	1,1	57,43,71,85,55	296	C21H44	Heneicosane	x	X	x	x	x
57,2	1,25	43,57,55,97,41	308	C22H44	1-n-docosene	x	X	x	x	-
57,3	1,15	57,71,85,55,56	310	C22H46	docosane	x	X	x	x	x
60,1	1,3	57,55,97,83,41	322	C23H46	tricosene	x	X	-	x	-
60,2	1,25	57,43,71,55,85	324	C23H48	tricosane	x	X	x	x	x
62,9	1,35	55,57,83,97,69	336	C24H48	1-n-tetracosene	x	X	-	x	-
63	1,3	57,71,55,41,85	338	C24H50	tetracosane	x	X	x	-	-
65,7	1,35	57,43,71,85,41	352	C25H52	pentacosane	x	X	x	x	x
68,3	1,4	57,71,85,44,41	366	C26H54	hexacosane	x	X	x	x	x
70,7	1,5	57,71,43,85,55	380	C27H56	heptacosane	x	X	-	x	x
73,1	1,55	57,43,71,85,55	394	C28H58	octacosane	x	X	-	-	-
75,5	1,6	57,71,43,85,55	408	C29H60	nonacosane	x	X	-	x	x
77,6	1,65	57,43,55,97,71	422	C30H62	triacontane	x	-	-	-	x
79,7	1,75	57,71,43,85,83	436	C31H64	hentriacontane	x	X	-	-	x
81,7	1,85	57,71,43,85,55	450	C32H66	dotriacontane	x	X	-	-	-

Other alkyl hydrocarbons

11	2,75	57,43,41,71,56	142	C10H22	substituted alkane	x	X	-	-	-
----	------	----------------	-----	--------	--------------------	---	---	---	---	---

14,4	3,4	55,41,43,56,69	154	C11H22	positional isomer undecene	x	x	x	-	-
14,7	3,3	57,43,71,41,56	156	C11H24	substituted alkane	x	x	-	t	-
18,6	4	41,55,43,56,69	168	C12H24	positional isomer dodecene	x	x	x	x	-
19	3,7	57,43,71,41,85	170	C12H26	substituted alkane	x	x	-	-	-
19,5	3,5	57,43,71,41,56	184	C13H28	Undecane, 2,6-dimethyl-	x	x	-	-	-
23,1	4,25	55,41,43,56,69	182	C13H26	Cyclotridecane/positional isomer tridecene	x	-	x	x	x
27,7	4,85	43,55,41,57,69	196	C14H28	Cyclotetradecane/positional isomer tetradecene	x	x	x	x	x
27,9	4,35	57,43,71,41,85	198	C14H30	substituted alkane	x	-	-	t	-
31,9	4,75	55,43,41,69,57	210	C15H30	cyclopentadecane/positional isomer pentadecene	x	-	x	x	x
32,3	4,5	57,43,71,85,41	212	C15H32	substituted alkane	x	-	x	x	x
36,1	5,4	43,41,55,57,83	224	C16H32	isomer of hexadecene	-	-	-	x	x
40,3	5,15	57,71,43,41,85	240	C17H36	substituted alkane	x	-	-	x	x
43,9	5,75	57,83,55,69,43	252	C18H36	isomer octadecene	x	-	-	-	-

Hopane structures

53,4	2,1	191,41,95,55,123	276	C20H36	NA	x	x	-	-	-
56,1	2,15	191,95,55,109,69	290	C21H38	NA	x	x	-	-	-
61,3	2,15	191,69,95,55,81	318	C23H42	NA	x	x	-	-	-
62,8	2,15	191,69,95,81,55	332	C24H44	15-Isobutyl-(13 α H)-isocopalane	x	x	-	-	-
65,9	2,25	191,69,95,55,81	346	C25H46	NA	x	x	-	-	-
68	2,25	191,95,81,69,109	360	C26H48	NA	x	x	-	-	-
68,2	2,25	191,95,55,192,81	360	C26H48	NA	x	-	-	-	-
68,6	2,95	191,67,81,95,109	402	C29H54	NA	x	-	-	-	-
72,9	2,4	191,57,69,81,95	388/402	C29H54	NA/ norhopane	x	x	-	-	-
73,1	2,4	191,69,43,81,95	388/412	C28H52/	NA /norhopane	x	x	-	-	-

					C30H52						
76,6	3,45	191,95,67,55,81	370	C27H46	NA/norhopane	x	x	-	-	-	
77,4	3,7	191,231,161,95,69	368	C27H44	NA	x	x	-	-	-	
77,6	3,6	191,95,81,149,69	370	C27H46	hopane/17 α (H)-22,29,30-trisnorhopane?	x	x	-	-	-	
80,4	3,55	191,137,177,69,81	398	C29H50	28-Nor-17 β (H)-hopane/17 α (H),21 β (H)-30-nor-hopane(384)	x	x	-	-	-	
81,3	3,65	191,355,192,67,137	398	C29H50	28-Nor-17 α (H)-hopane?	x	x	-	-	-	
81,8	3,55	191,95,123,192,81	412	C30H52	Gammacerane	x	x	-	-	-	
82	3,75	191,69,121,149,192	410	C30H50	A'-Neogammacer-22(29)-ene?	x	x	-	-	-	
85,3	4,9	191,69,95,192,81	412	C30H52	NA	x	x	-	-	-	

Aromatic steroid structures

69,2	2,9	253,44,254,143,207	336?	NA	NA	x	x	-	-	-
71,3	3	253,254,143,252,43	NA	NA	NA	x	x	-	-	-
73	3,05	253,254,143,252,267	NA	NA	NA	x	x	-	-	-
74,8	3,15	253,254,44,143,207	NA	NA	NA	x	x	-	-	-
76,5	3,3	253,254,207,218,451	NA	NA	NA	x	x	-	-	-

**Groups I-V markers compounds
Group I**

16	5,9	119,134,133,91,120	134	C10H14	Benzene, 1,2,4,5-tetramethyl-	x	x	-	-	-
17,5	0,4	119,134,120,91,118	134	C10H14	Benzene, 1,2,3,4-tetramethyl-	x	x	-	-	-
17,5	1,4	119,134,120,117,133	134	C10H14	Benzene, 1,2,3,4-tetramethyl-	x	x	-	-	-

17,5	3,45	119,134,91,118,77	134	C10H14	Benzene, 1,2,4,5-tetramethyl-	x	x	-	-	-
17,5	4,1	119,134,117,91,118	134	C10H14	Benzene, 1,2,4,5-tetramethyl-	x	x	-	-	-
17,5	5,56	119,91,134,92,44	134	C10H14	NA	x	x	-	-	-
17,7	1,15	130,115,129,128,63	130	C10H10	1H-Indene, 3-methyl-	x	x	x	-	-
18,1	1,95	128,127,129,64,63	128	C10H8	Naphthalene	x	x	x	-	-
18,2	2	105,134,133,77,119	134	C9H10O	Benzaldehyde, 4-ethyl-	-	-	x	-	-
18,4	1,85	130,129,115,128,131	130	C10H10	2-Methylindene	x	x	x	-	-
18,6	2,15	119,91,134,65,43	134	C9H10O	Ethanone, 1-(3-methylphenyl)-	-	-	x	-	-
19,5	2,1	128,57,127,129,43	128	C10H8	1H-Indene, 1-methylene-	x	x	x	x	x
19,9	1,95	121,136,91,58,135	136	C9H12O	Phenol, 2,4,5-trimethyl-	x	x	x	-	-
21,1	2,5	119,91,148,117,105	148	C11H16	Benzene, 1-methyl-4-(1-methylpropyl)-	-	x	-	-	-
21,8	1,35	91,104,117,105,92	160	C12H16	Benzene, 4-hexenyl-	-	-	-	-	-
22,2	0,75	91,92,162,41,105	162	C12H18	Benzene, hexyl-	-	-	-	-	-
22,3	2,05	119,148,91,120,147	148	NA	NA	-	-	-	-	-
Group II										
22,5	1,9	129,144,128,130,143	144	C11H12	1H-Indene, 4,7-dimethyl-	x	x	x	x	x
22,9	1,95	129,144,128,130,127	144	C11H12	1H-Indene, 2,3-dimethyl-	x	x	x	-	-
23	2,1	141,142,71,115,139	142	C11H10	Benzocycloheptatriene	x	-	x	-	-
23,9	2,1	129,144,128,127,115	144	C11H12	1H-Indene, 1,3-dimethyl-	x	x	x	-	-
24,1	2,1	129,144,128,127,143	144	C11H12	1H-Indene, 1,1-dimethyl-	x	x	x	-	-
24,4	2,3	142,141,115,143,39	142	C11H10	Naphthalene, 2-methyl-	x	-	x	x	x
24,5	2,4	147,148,141,44,142	148	C9H8S	Benzo[b]thiophene, 5-methyl-	x	x	-	-	-
25,1	2,9	142,141,115,143,58	142	C11H10	Naphthalene, 1-methyl-	x	x	x	-	-
25,1	3,5	148,147,149,115,73	148	C9H8S	Benzo[b]thiophene, 6-methyl-	x	x	x	-	-
25,2	2,4	142,141,115,70,143	142	C11H10	1H-Indene, 1-ethylidene-	x	x	x	x	x

	25,2	2,7	141,142,140,115,143	142	C11H10	NA	x	-	x	-	-
Group III											
	26,5	2	143,128,158,129,142	158	C12H14	1H-Indene, 1,1,3-trimethyl-	x	x	x	-	-
	27,1	2	143,128,158,142,141	158	C12H14	1H-Indene, 1,2,3-trimethyl-	x	x	x	-	-
	27,3	1,95	158,143,128,159,44	158	C12H14	Benzene, p-diisopropenyl- Benzene, 1,3,5-trimethyl-2-	x	x	x	-	-
	27,6	2	143,158,128,115,144	158	C12H14	(1,2-propadienyl)-	x	x	x	x	-
	27,63	0,7	143,128,158,129,144	158	C12H14	1,2,3-Trimethylindene	-	-	-	-	x
	28,7	2,15	143,128,158,141,142	158	C12H14	1H-Indene, 1,1,3-trimethyl-	x	x	x	x	-
	28,6	2,4	162,161,163,147,128	162	C10H10S	Benzo[b]thiophene, 3,6- dimethyl-	x	x	-	-	-
	28,6	2,85	162,161,163,147,128	162	C10H10S	Benzo[b]thiophene, 2,7- dimethyl-	x	x	-	-	x
	29,6	3,25	162,161,163,147,115	162	C10H10S	Benzo[b]thiophene, 2,5- dimethyl-	x	x	-	-	-
	29,3	2,45	156,141,155,157,115	156	C12H12	Naphthalene, 2,7-dimethyl-	x	x	x	x	-
	29,4	2,35	156,141,155,77,44	156	C12H12	Naphthalene, 1,5-dimethyl-	x	x	x	-	-
	29,9	2,45	156,141,155,157,77	156	C12H12	Naphthalene, 1,7-dimethyl-	x	x	-	-	x
	29,9	2,8	156,141,155,63,157	156	C12H12	Naphthalene, 1,6-dimethyl-	x	x	x	-	-
	30,1	2,8	156,141,155,66,157	156	C12H12	Naphthalene, 1,3-dimethyl-	x	x	x	x	-
	31,1	1,55	91,104,92,117,105	188	C14H20	Benzene, 1-octenyl-	-		x	-	-
	31,4	1,4	92,91,190,93,57	190	C14H22	Benzene, octyl-	-		x	-	-
	31,5	3,45	156,141,155,115,142	156	C12H12	Naphthalene, 1,2-dimethyl-	x		-	-	-
Group IV											
	33,6	2,35	155,170,127,84,56	170	C13H14	Naphthalene, 1,4,6- trimethyl-	x	x	x	-	-
	33,6	2,95	176,161,175,177,160	176	C11H12S	Benzo[b]thiophene, 2,5,7- trimethyl-	x	x	-	-	-
	33,76	2,35	155,170,154,153,171	170	C13H14	3-(2-Methyl-propenyl)-1H- indene	-	x	-	x	x
	34,2	3,4	161,176,175,177,160	176	C11H12S	Benzo[b]thiophene, 2-ethyl- 5-methyl-	x	x	-	-	-

34,4	2,75	170,155,169,152,154	170	C13H14	Naphthalene, 2,3,6-trimethyl-	x	x	-	x	x
34,7	2,65	170,155,169,156,154	170	C13H14	Naphthalene, 1,6,7-trimethyl-	x	x	x	x	x
34,9	3,55	176,161,175,162,177	176	C11H12S	Benzo[b]thiophene, 7-ethyl-2-methyl-	x	x	-	-	-
35	3,35	176,161,175,165,45	176	C11H12S	Benzo[b]thiophene, 2,5,7-trimethyl-	x	x	-	-	-
35,3	3,05	170,155,156,152,76	170	C13H14	3-(2-Methyl-propenyl)-1H-indene	x	x	-	-	-
35,5	2,9	170,155,156,152,154	170	C13H14	isomer of naphthalene, trimethyl-	x	x	x		x
35,7	1,45	92,91,204,93,45	204	C15H24	Benzene, nonyl-	-	-	x	x	x
36,8	3	175,190,176,174,177	190	C12H14S	Benzo[b]thiophene, 2-ethyl-5,7-dimethyl-	x	x	-	-	-
37,4	2,85	161,175,44,175,162	190	C12H14S	/Benzo[b]thiophene, 2,7-diethyl-	x	x	-	-	-
40,03	1,45	92,91,93,218,43	218	C16H26	Benzo[b]thiophene, 2,3-diethyl-	-		-	x	x
41,1	1,15	105,106,91,232,92	232	C17H28	Benzene, decyl-	-		-	x	x
42,6	1,6	119,120,91,105,232	232	C17H28	Benzene, (1-methyldecyl)-	-		x	x	x
43,9	1,6	92,105,91,106,232	232	C17H28	Benzene, (1,1-dimethylnonyl)-	-		x	x	x
44,1	3,6	184,185,183,152,92	184	C12H8S	Benzene, undecyl-	-		x	x	x
47,7	3,55	198,197,199,198,85	198	C13H10S	Dibenzo[b,d]thiophene	x	x	-	-	-
48,4	3,6	198,197,199,98,45	198	C13H10S	Dibenzothiophene, 3-methyl-	x	x	-	-	-
49,2	3,85	198,197,199,165,100	198	C13H10S	Dibenzothiophene, 3-methyl-?	x	x	-	-	-
51,8	3,55	212,211,165,105,163	212	C14H12S	Dibenzothiophene, 4-methyl-2,8-Dimethyldibenzo(b,d)thiophene/2,6-Dimethyldibenzothiophene/2,7-Dimethyldibenzothiophene	x	x	-	-	-

52,6	3,75	212,211,197,213,106	212	C14H12S	1,7-Dimethyldibenzothiophene	x	x	-	-	-
60,6	3,9	240,225,219,234,241	240	C16H16S	Dibenzo[b,d]thiophene, 1,3,6,7-tetramethyl-	x	x	-	-	-
68,7	5,3	248,247,249,123,124	248	C17H12S	3-Methylphenanthro[9,10-b]thiophene	x	x	-	-	-
71,8	5,35	262,43,123,245,261	262	C18H14S	Benzo[b]naphtho[2,3-d]thiophene, 6,8-dimethyl-	x	x	-	-	-
Group V										
45,1	3,65	178,177,89,176,179	178	C14H10	phenanthrene	-	x	x	-	-
45,2	3,6	178,177,89,176,179	178	C14H10	phenanthrene	x	x	x	-	-
49,4	3,6	192,191,96,193,189	192	C15H12	Phenanthrene, 3-methyl-	x	x	x	-	-
50	3,75	192,191,189,83,94	192	C15H12	Anthracene, 1-methyl-	x	x	x	-	-
50,1	3,7	192,191,83,193,95	192	C15H12	Phenanthrene, 4-methyl-	x	x	x	-	-
50,2	3,75	192,191,96,95,193	192	C15H12	Anthracene, 9-methyl-	x	x	x	-	-
53,7	3,55	206,191,205,44,89	206	C16H14	9,10-Dimethylanthracene	x	x	x	-	-
57,1	3,65	220,205,210,202,204	220	C17H16	Phenanthrene, 2,3,5-trimethyl-	x	x	-	-	-
57,4	3,65	220,44,221,219,189	220	C17H16	Phenanthrene, 2,3,5-trimethyl-	x	x	-	-	-
60	4,1	220,205,104,202,101	220	C17H16	Phenanthrene, 2,3,5-trimethyl-	x	x	-	-	-
61,1	4,75	216,215,108,213,95	216	C17H12	isomer Pyrene, methyl-	-	x	x	-	-
61,3	4,7	216,215,95,217,43	216	C17H12	Pyrene, 1-methyl-	x	x	x	-	-
64,2	4,6	230,44,215,43,229	230	C18H14	isomer of Pyrene, dimethyl-	x	x	-	-	-
64,5	4,7	230,215,231,113,229	230	C18H14	Pyrene, 1,3-dimethyl-	x	x	-	-	-
65,1	4,85	230,229,231,101,40	230	C18H14	isomer of Pyrene, dimethyl-	x	x	-	-	-
65,4	4,85	230,231,229,201,106	230	C18H14	isomer of Pyrene, dimethyl-	x	x	-	-	-

^a NA non assigned, ^b x present – absent